Submitted to SOLMAT

PV SOILING AND CLEANING: INITIAL OBSERVATIONS FROM 5-YEAR PHOTOVOLTAIC GLASS COATING DURABILITY STUDY

*Sarah Toth,*ˇ Matthew Muller,ˇ David C. Miller,ˇ Helio Moutinho,ˇ Bobby To,ˇ Leonardo Micheli,ˇ Jeffrey Linger,ˆ Chaiwat Engtrakul,ˇ Asher Einhorn,ˇ Lin Simpsonˇ*

ˇ National Center for Photovoltaics, National Renewable Energy Laboratory, Golden, CO 80401-3214
ˆ National Bioenergy Center, National Renewable Energy Laboratory, Golden, CO 80401-3214

**Corresponding author*: Sarah.Toth@nrel.gov +1 3032754887 https://www.nrel.gov/pv/accelerated-testing-analysis.html

ABSTRACT

The contamination of solar photovoltaic cover glass can significantly reduce the transmittance of light to the surface of the photovoltaic cell, reducing the module's power output. The solar industry has been developing antireflection (AR) and antisoiling (AS) surface coatings to enhance light transmittance and mitigate the impacts of soiling. Although uncoated glass has been field tested for decades, minimal data exist to demonstrate the durability of AR and AS coatings against abrasion and surface erosion, including from: natural weathering, airborne sand, and industry cleaning practices. Coupons 75 mm square of varying types have been field-deployed to gather long-term data on coating durability; the initial results are presented here after 1 year of outdoor exposure near Sacramento, California. Duplicate sets of coupons were cleaned monthly per four different cleaning practices. All coupons demonstrated inorganic soiling as well as microscale biological contamination, regardless of cleaning method. Additionally, full-sized, field-aged modules from other areas of the world presented with similar types of contamination as the field-aged coupons; micrographs and results from genomic sequencing of this contamination are included here. Optical microscopy, scanning electron microscopy, atomic force microscopy/energy-dispersive spectroscopy, surface roughness, transmittance, and surface energy analysis of representative specimens and cleaning practices are presented.

KEYWORDS

Coatings, durability, fungi, optical performance, particulate matter, soiling

1. INTRODUCTION

Solar photovoltaic (PV) module technology is projected to increase to the terawatt scale in the coming years [1]. Although numerous PV technologies continue to approach their theoretical Shockley-Queisser conversion efficiency limit, all technologies are susceptible to performance losses over time due to numerous failure modes, including cover-glass degradation [2]. One type of cover-glass degradation is soiling, or the deposition of ambient particulate matter (PM) onto the surface of solar glass. Losses due to soiling depend strongly on location, because ambient particulate matter is generated by both natural and anthropogenic sources and can vary due to factors such as climate, seasonal changes, soil composition, and proximity to industrial activities [3]. PV power losses from soiling have been reported from single-digit percentages to as high as 70% depending on the world location, often having a higher impact on annual PV performance than cell degradation [4] [5] [6] [7]

[8] [9] [10] [11] [12] [13]. Annual soiling losses in California have been observed to be in the 4%–7% range [2] [5] [6] [14]. Some of the concepts and findings in this study may be applied to other solar technologies, including concentrated solar power (CSP) [15].

The expected composition of soiling on the surface of PV modules will vary with the airborne particulate matter generated by both local and distant sources. Generally, soiling is primarily composed of silica particulates and the metal oxides commonly found in the Earth's crust. It can also include air pollutants such as soot, salts, and sulfuric acid particulates, the latter of which can be formed by gas-to-particle conversions in the atmosphere. Finally, biofilms, likely deposited onto the surface of a module as biological aerosols, can grow on solar glass [16]. Fungal and algal biofilms have previously been found on solar modules deployed in Sao Paulo, Brazil, that showed a 7% power loss within a 1-year period [17]. Biofilms are thought to interact and bind with the substrate in many ways, secreting organic acids and other compounds that may contribute to weathering and absorbing and scattering light [18]. Biofilm communities have been shown to work together to retain water and ambient particulates to satisfy their need for nutrients [19].

Currently, there is no systematic mitigation strategy for the soiling problem. It is common to monitor the degradation in system power output (due to soiling) and then to clean the modules when the economic gains outweigh the cost of cleaning [20]. Cleaning frequencies and methods depend on several factors, including the installation location. For example, in locations with regular rainfall, the system owner might rely solely on natural cleaning. In the southwest United States, there can be dry periods lasting 3–9 months, where the system owners perform 1–2 cleanings during these times. Water cleaning (by either pressurized spray or wet brushing) is typical in the southwest United States. In desert regions of the Middle East, where water is scarce or expensive, dry cleaning with a brush is often used. Various types (both wet and dry) of automated cleaning robots are also being introduced to the marketplace. Standard solar modules with a glass front have been deployed in various field conditions for decades. Therefore, solar glass is generally accepted as sufficiently durable to cleaning practices. In recent years, surface coatings have been applied to solar glass, but it is not known how durable these coatings are to natural weathering or cleaning. For example, many manufacturers now include AR coatings on the glass surface to boost module performance on the order of 3% [21]. In response to the soiling problem, there is significant effort underway to develop AS coatings or surface functionalizations that will help maintain clean module surfaces [22] [23] [24] [25]. With the advent of these coatings, it has become an industry priority to develop standardized durability testing to determine if coatings will be economically viable under various field environments or cleaning practices [21].

The National Renewable Energy Laboratory (NREL) is currently working with industry to develop standardized durability test methods for surface coatings for PV modules. As part of this work, a 5-year field experiment is underway to collect coating degradation data from the field. The primary goal of the study is to collect abrasion and damage data to validate accelerated abrasion tests. Multiple coating types as well as baseline solar glass have been deployed at five challenging world locations. Various options for cleaning the coatings are being studied systematically to represent normal industry practices, including: 1) no clean, 2) low-pressure wet

spray with no mechanical contact, 3) wet sponge wipe followed by a squeegee, and 4) dry brushing. This protocol is also expected to provide insight about the abrasion due to cleaning practices, natural weathering damage, the mechanisms enabling soiling, site-specific soiling differences, and the performance and durability of the different coating types. This paper presents selected results from the first set of samples that were collected after being deployed in a rural area bordering Sacramento, California, for 1 year. Results will also be compared to specimens obtained from a module deployed in Argenbühl, Germany, for 6 years and Palms, California, for 11 years.

2. METHODS

In this study, ten types of 75-mm × 75-mm coated or uncoated samples—or "coupons"—were deployed to weather for 1–5 years in or near the cities of Sacramento, California; Tempe, Arizona; Dubai, U.A.E; Mumbai, India; and Kuwait City, Kuwait. Each location represents a unique climate and soiling potential (Table 1): the Sacramento location is in an agricultural area with the potential for a long dry season as well as wetter periods; the Tempe location is east of Phoenix in a suburban environment near the dry Arizona desert; the Mumbai location is an urban environment and is known for a long dry period and a monsoon season; the UAE location is in the desert south of Dubai where frequent coastal dew cycles occur; finally, the Kuwait city location is a dry desert environment with a high frequency of sandstorms. Also included in Table 1 are two locations where full-sized PV modules were aged; some observations regarding those modules are reported in this paper.

Table 1. Coupon deployment locations, respective climate classifications, PM2.5 concentrations, dust storm, and precipitation information [26] [27] [28]. PM2.5 represent estimates of the average ground-level concentration (in $\mu g/m^3$) of fine particulate experienced in 2015 by each site. These data have been extracted from the 0.1-degree × 0.1-degree resolution database developed by [29].

Deployment Location: City, State (Country)	Köppen Climate Classification	General Climate Type	Average PM2.5 ($mg \times m^{-3} \times y^{-1}$)	Number Dust Storms (y^{-1})	Annual Precipitation (mm)
Sacramento, CA (USA)	Csa	Mediterranean	14.9	0	464
Tempe, AZ (USA)	BWh	Hot desert	12.6	4	204
Mumbai (India)	Aw	Tropical wet & dry	52.5	0	2,258
Dubai (UAE)	BWh	Hot desert	86.4	4	94
Kuwait City (Kuwait)	BWh	Hot desert	70.8	21	116
Argenbühl (Germany)	Cfb	Temperate oceanic	10.0	0	1,159
Palms, CA (USA)	Csa/Csb	Mediterranean	10.5	0	379

The coupons are mounted on racks at a 30-degree tilt in Sacramento, Tempe, and Kuwait City, whereas they are inclined at 25 degrees in Dubai and 19 degrees in Mumbai. All racks are installed on the ground except for Mumbai, which is on a rooftop within the city. Figure 1 is an image of the coupons as installed in Sacramento, California, and they are the first samples to achieve a year in the field; therefore, they are the focus of this paper.

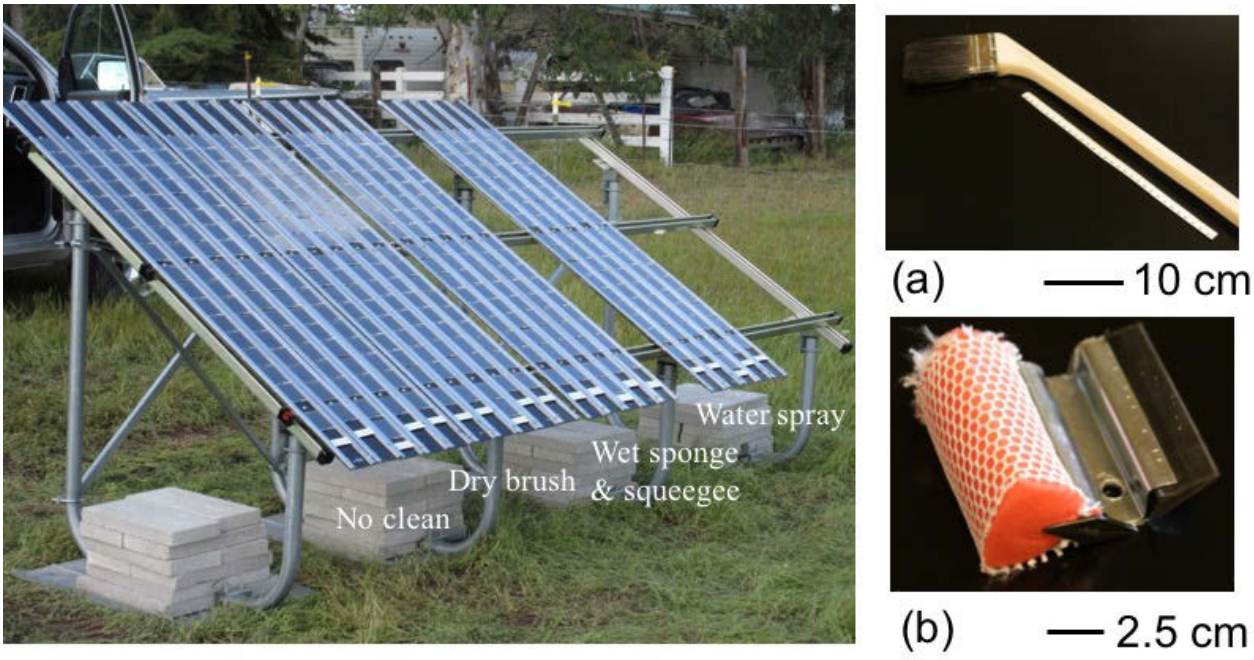

Figure 1: A 30-degree tilt rack with 20 coupon holders (each holding seventeen 75 mm × 75 mm coupons) as deployed outside Sacramento, California in April 2016. From left to right, the first coupon holders are never cleaned; the coupons in the next five holders are dry brushed monthly, the next five are rubbed with a wet sponge followed by a squeegee monthly, and the last five are water sprayed monthly. One coupon holder is removed from each set of cleaning methods each year and returned to NREL for each of the 5 years in the study. Figure 1 (a) shows a representative brush (with horse hair bristles) used for dry brush cleaning; Figure 1 (b) shows a representative head for a squeegee used with water.

The coupons (see Figure 1) in this study are 75 mm × 75 mm and are all coated or uncoated float glass substrates except for one plastic sample, poly(methyl methacrylate) (PMMA), which is representative of lenses that have been used in concentrator PV modules. NREL provided Diamant 3.2-mm-thick, low-iron float glass (by Saint-Gobain S.A.) to various collaborators in the coating industry as a common substrate material. One coating manufacturer instead used 3.2-mm-thick Optiwhite float glass (Pilkington Group Ltd.) as the substrate material. To have a comparison to the coatings, uncoated Diamant and Optiwhite glass coupons were deployed. Because solar modules typically have tempered glass, a set of heat-tempered, uncoated Diamant glass coupons were also deployed. In some cases, manufacturers put their coatings through a heat-treatment process, but none were subjected to the full tempering procedure that is expected of commercial PV modules. Each coupon was scribed with a letter and three-digit number; the letter represents the specimen or coating type (as described in Table 2) and the number is for sample tracking. Coupons J and T are uncoated Diamant glass reference, with T being a tempered version. Coupons K are uncoated Optiwhite reference glasses. Coupons B, D, H, U, E, and G are various coatings (AR, AS, hydrophilic, or hydrophobic) that were deposited by the manufacturers on reference glass substrates. “A” coupons consist of 3-mm-thick, uncoated PMMA. All coupons except for E, G, and K have

duplicates deployed in each holder in case of damage. Due to the large quantity of data for the complete set of samples, only results from certain coupons are presented here to support the major findings of this study.

To simulate the various cleaning practices currently in use, one set of holders is never cleaned except for natural events such as rain, wind, or dew while the others are cleaned monthly by either a dry brush, wet sponge and squeegee, or low-pressure water spray. The water used in cleaning did not contain a surfactant or anti-spotting agent. The brush was composed of hog bristle and the sponge and squeegee were polyethylene and rubber.

Table 2. Characteristics of all indexes of 75 × 75 mm coupons. Two types of AR coatings were used in this study: a graded index (where the refractive index was varied through thickness of the coating based on its porosity) and a single-layer interference coating (where destructive interference minimizes reflection at an optimal wavelength; i.e., a quarter-wave layer) [30]. Hydrophobicity was determined by the water contact angle; $10° < \theta \leq 55°$ was designated hydrophilic, $55° < \theta \leq 90°$ was designated weakly hydrophilic, and $90° < \theta \leq 120°$ was designated weakly hydrophobic.

Index	Substrate Material	AR Type	AS Functionality?	Hydrophobicity
A	PMMA	N/A	N/A	Weakly hydrophilic
B	Diamant	Graded index	Y	Weakly hydrophobic
D	Diamant	Graded index	Y, oleophobic	Weakly hydrophilic
E	Optiwhite	Graded index	N/A	Hydrophilic
G	Optiwhite	Graded index	Y	Hydrophilic
H	Diamant	Interference	Y	Weakly hydrophobic
J	Diamant	N/A	N/A	Hydrophilic
K	Optiwhite	N/A	N/A	Hydrophilic
T	Diamant, tempered	N/A	N/A	Hydrophilic
U	Diamant	Interference	Y	Weakly hydrophobic

AluPOLY (Piedmont Plastics Co.), an ultraviolet durable black lacquer/aluminum/polyethylene core/aluminum/black lacquer composite for use in the outdoor sign industry, was used as the back plate behind the coupons to raise the temperature of the samples to be representative of dark solar cells behind cover glass. It was also used to cover the coupons to protect the surfaces from additional contamination during the shipping process. After 1 year in Sacramento, California, a holder from each cleaning set was removed, individually covered, and shipped to NREL in a padded plywood container. Upon arrival, the coupon holders were checked for observable damage that may have occurred during the shipping and handling process. Only one coupon was found to be broken, B178, but its duplicate was intact.

Coupons were characterized using various techniques: optical microscopy was performed on a SMZ-1500 Zoom Stereo Microscope (Nikon Instruments Inc.) equipped with a DS-Fi1 camera (Nikon Instruments Inc.).

Optical surface profilometry was conducted on a VEECO WYKO NT1100 (Bruker Corp.) using vertical scanning white-light interferometry with a 20x objective to map the surface roughness of coupons; as per the manufacturer, the z-resolution of this instrument in this mode is < 1 nm. A Lambda 1050 spectrophotometer (Perkin-Elmer Inc.) was used to collect hemispherical (150-mm InGaAs Integrating Sphere attachment) and direct (3D WB Det Module attachment) transmittance data. The angle of acceptance for direct measurements is estimated to be on the order of ±2°–3° [31]. The representative solar-weighted photon transmittance (rSWT) (for the wavelength range from 300 to 1250 nm, as in contemporary flat-panel PV devices) as well as the diagnostic characteristics of SWT (from 280 to 2500 nm), yellowness index, and UV cut-off wavelength were calculated from the transmittance spectra according to IEC 62788-1-4 [32] [33]. Contact angles of three different chemicals—deionized water (DIW), diiodomethane (CAS 75-11-6), and formamide (CAS 75-12-7)—were measured on a 100-25-A goniometer (Ramé-Hart Instrument Co.) to measure changes in surface energy. The different probe liquids are intended to highlight the contributors to surface energy including polar (water), dispersive (diiodomethane), and acid/base (formamide) interactions. Measurements were typically performed for three replicate specimens or three separate measurements on different locations within the same coupon.

All coupon types were baselined per each measurement procedure before field deployment. Samples were removed from the holder and their backside was wiped with a dampened soft cloth to remove contamination trapped between the sample and the holder backplate before optical imaging and other characterization. For some cases, it was relevant to take measurements after loose soil was removed or after the surface was more fully cleaned. Since loose soiling may have unevenly shaken off the coupons during the shipping process, any remainder was removed by a 5-second rinse with laminar-flow DIW, followed by a 10-second compressed-air spray. To more fully clean samples, a wiping process was used that included a 1-minute wipe with a DIW-saturated WypAll X60 towel (Kimberly-Clark Corp.). In later figures, “R” denotes that the coupon was measured after the 5-second rinse and “W” denotes the coupon was measured after the 1-minute wipe. Uncoated specimens examined using scanning electron microscopy (SEM) were cleaned using a non-contact cleaning procedure, Standard Clean 1 (SC-1): 10 minutes of sonication in DIW with a mild Liqui-Nox surfactant (Alconox Inc.) followed by a 10-minute soak in a 10% ammonia, 10% peroxide solution.

In addition to the standard characterizations, SEM and atomic force microscopy (AFM) were performed on certain samples. The SEM micrographs were taken using a field-emission FEI Nova NanoSEM 630, in secondary-electron mode. The AFM used in the analysis was a Bruker Dimension 3100 with Nanoscope V controller, using Si probes in non-contact mode. Certain optical images were taken using a Zeiss AXIO Imager.M2m optical microscope in reflection mode.

In addition to the coupon coatings study, field-aged, full-sized PV modules have been shipped to NREL from various locations around the world. Two modules of note are included in this report for comparison to the findings from the coupon study: one module from Argenbühl, Germany (used for 6 years), and another from Palms, California (used for 11 years). Optical microscopy was first performed on the as-received modules using the same Nikon microscope as in the coupon coating study. The contamination on these modules went through

the same rinse and wipe process described for the coupons above, as well as an up-close pressure wash using DIW. Images of fungal growth (Figures 17b and 17d) were collected on a digital microscope (Keyence; VHX-5000) over a magnification range of 100 to 1000x (Keyence; VH-Z100R). In addition, glare was suppressed by using two polarization adaptors (Keyence; OP-72406 and OP-87800). After initial characterization, the field modules were broken to facilitate subsequent examination using shards of the front glass.

The fungi on the field-aged module from Argenbühl, Germany were cultivated directly from the module's glass shards for identification. A rich growth medium, Yeast Mold (YM) broth (3 g/L yeast extract, 3 g/L malt extract, 10 g/L dextrose, 5 g/L peptone, pH 3.5), was used. The broth was designed to enrich for yeast and fungal species while being growth inhibitory for most bacterial species. Glass shards from the Argenbühl module were used to directly inoculate 5 mL of YM broth in a glass culture tube that was grown at 30°C using a New Brunswick Roller Drum. Following 3 days of growth, the entire 5 mL mixture (including the shard) was used to inoculate 25 mL of YM broth in 125 mL non-baffled Erlenmeyer flasks. Cultures were incubated at 30°C with 100 RPM shaking for seven days. In order to identify the contaminating fungus, a fungal mass (~100 mL) was isolated and sent to Genewiz (South Plainfield, NJ) for extraction and sequencing of the genomic DNA of the Internal Transcribed Spacer (ITS) region.

3. RESULTS AND ANALYSIS

3.1 Filamentous fungi

All coupons had a layer of soiling that was just above the threshold of visual observation. Optical microscopy revealed root-like structures emanating from concentrations of particles located about a central mass on all coupons, regardless of cleaning method or coating type. Microscopy of as-received and post-rinse surfaces identified that virtually none of the contamination was removed through cleaning by rinsing (Figure 2).

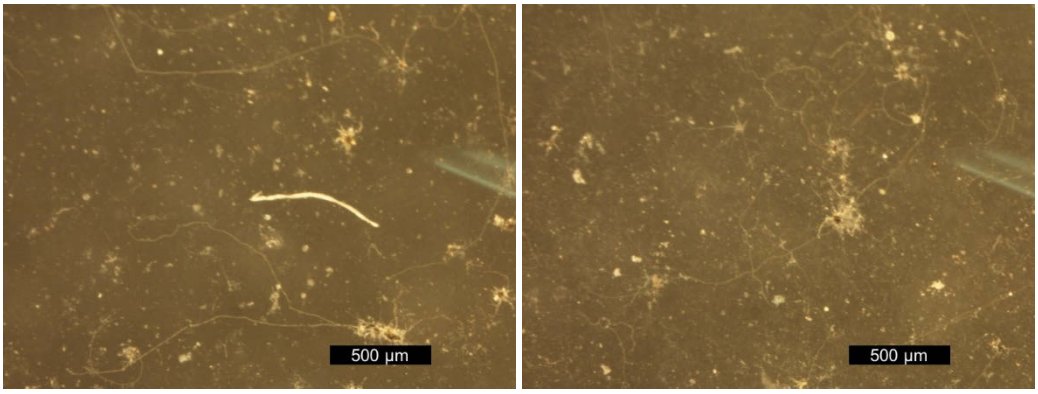

Figure 1: Micrograph of a water-sprayed T coupon (Diamant baseline tempered glass with no coating), as-received (left) and rinsed (right), showing particulates and the root-like filaments of the fungi. Most of the particulate matter and soiling as well as fungi remain after the 5-second rinse. Background tint results from the microscope stage, and the chromatic artifact in the right of each image is a reflection of the ambient fluorescent lighting.

Figure 3 shows an SEM image of one of the fungal growths. There is clearly a higher concentration of particulates on and around the central structure of the fungi, as well as the fungal filaments.

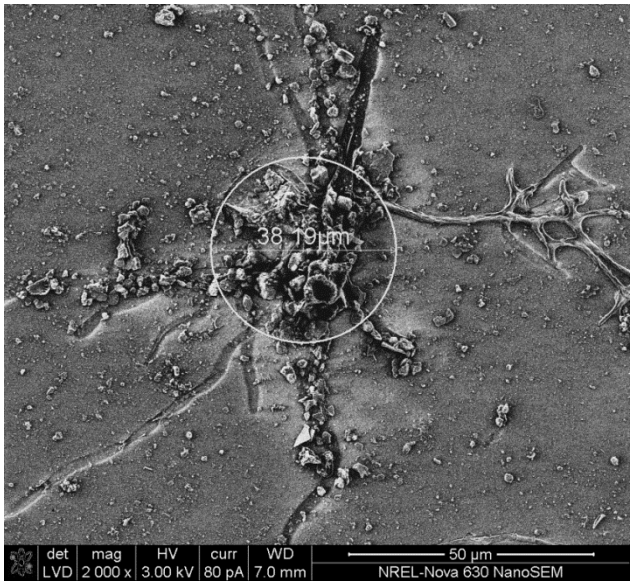

Figure 3: SEM image from the same coupon shown in Figure 2. The fungi centroid spans about 38 µm in diameter.

Some of the filaments in Figure 3 appear as if they are above the glass substrate whereas others appear recessed into the glass. References dating back as far as 1924 and including [34] [35] [36] [37] [38] suggest that fungi and bacteria can etch and pit glass. Further SEM and AFM investigations were conducted to clarify if glass etching had occurred here. SC-1 was used on a no-clean K coupon (uncoated Optiwhite glass) to remove the growths without abrading or further affecting the coupon surface. Prior to the cleaning, a cross was scribed on the glass surface to identify examination locations both before and after the non-abrasive cleaning. Figure 4 shows an optical image with associated dimensions for the fungi before cleaning. AFM line scans were measured for various features in locations a–d of Figure 4; various sizes of particles and fungi were found, but no concavity (into the glass substrate) was observed. The glass was then cleaned using SC-1; the majority of particulates and fungi are shown to be removed.

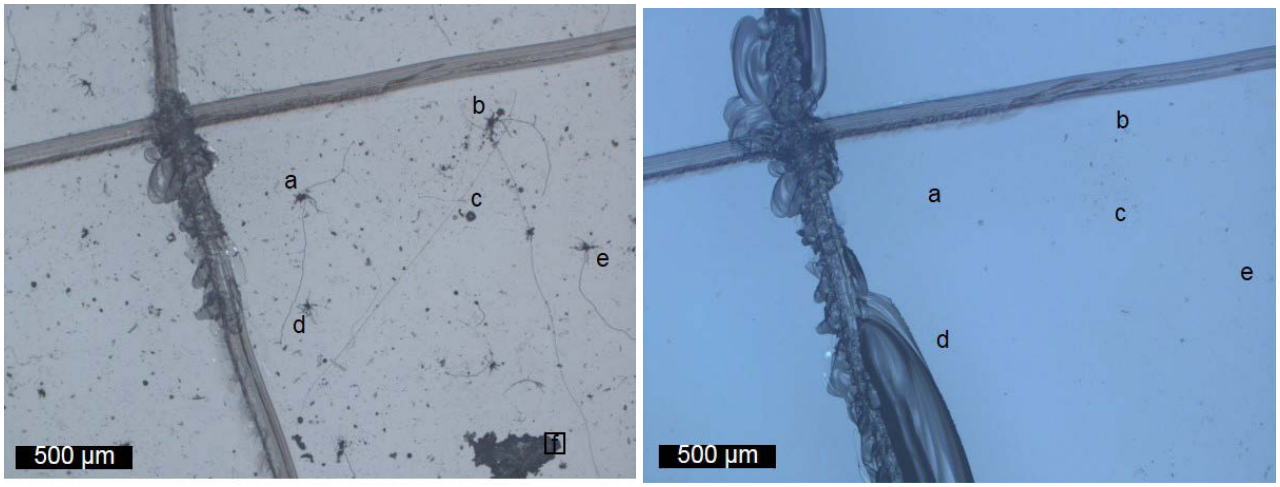

Figure 4: An optical image with indication of the locations of various fungi before (left) and after (right) the cleaning of coupon NC K198. The fungi at locations a–d have been removed, while only minor surface contamination remains on the specimen. Note that at location d the scribe is itself affected by cleaning. Differences in the cross used to mark the location of examination are attributed to the sonication during the cleaning process.

SEM (Figure 5) and AFM measurements after cleaning showed no evidence of surface recessions in the locations a–d; i.e., no evidence of glass etching was observed.

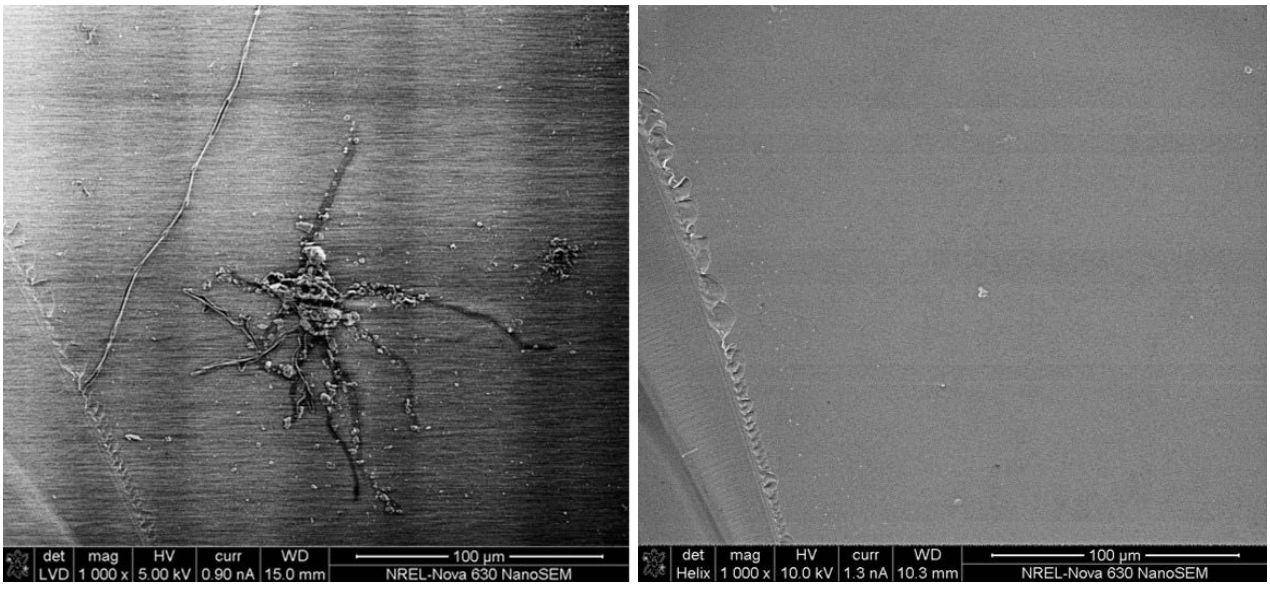

Figure 5: SEM images of location d in Figure 4 before (left) and after (right) cleaning with SC-1.

Figure 6 presents two SEM images for location b from Figure 4. Specific particles or portions of the fungi are identified within the SEM images by numbers 1-4. The EDS elemental analysis of these four locations is provided in Table 3, which shows that there are differences in the composition of contamination across the sample.

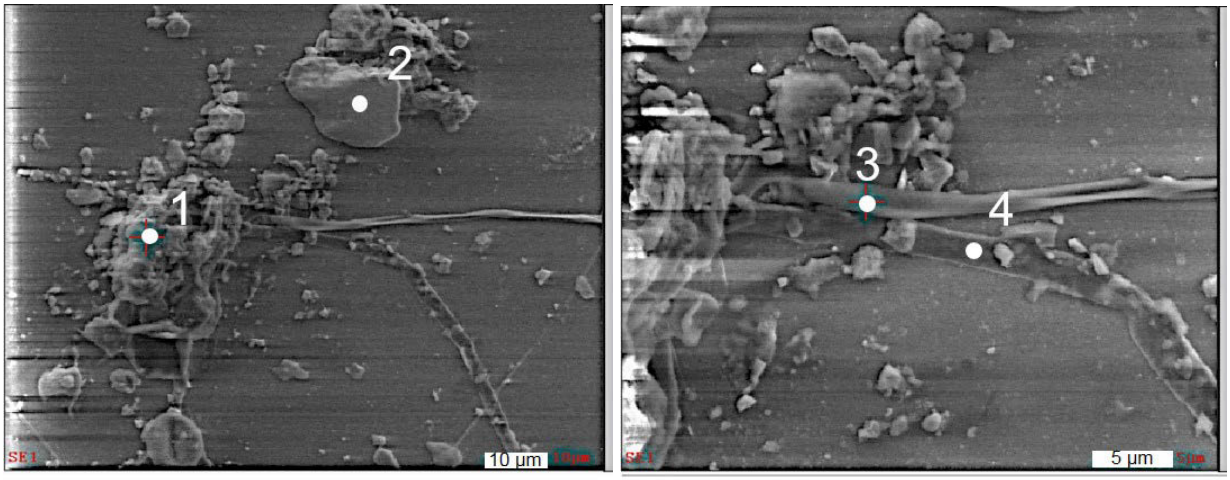

Figure 6: Specific SEM images from location b in Figure 4. Numbered locations on these SEM images were subject to EDS elemental composition analysis; results shown in Table 3.

Table 3. Elemental composition of the locations identified in Figure 6.

Position	Elemental Composition from EDS (%)									
	C	O	Fe	Na	Mg	Al	Si	Cl	K	Ca
1	30.7	36.1	–	5.5	1.8	0.7	21.2	0.5	0.7	2.4
2	6.4	45.6	1.4	7.2	3.5	3.1	29.8	–	–	3.1
3	20.3	38.7	–	7.0	2.1	0.8	28.0	–	–	3.1
4	10.4	43.1	–	7.7	2.4	1.2	31.9	–	–	3.4

The fungal contaminants were cultivated directly from shards of a field-aged module (Argenbühl, Germany) in YM broth for identification. Briefly, glass shards showing microscopic evidence of fungal contamination were used to inoculate 5 mL YM broth in glass culture tubes. During this period, there was clear microbial growth associated with the shard observable after day three; additionally, a spherical pellet of apparent fungal origin had detached from the fungal mass associated with the shard (Figure 7, top left). Following this initial growth, the media, the glass shard, and the spherical fungal pellet were transferred to a 125 mL flask containing 25 mL of YM broth. Strikingly, the fungal mass associated with the shard had completely encapsulated the shard by day 7 (Figure 7, top right). On day 7, the fungal mass was isolated from the liquid media and the glass shard was extracted (Figure 7, bottom left and bottom right). Additional glass shards from the field-aged module (Argenbühl, Germany) were placed into Luria Broth (LB) to enrich for bacteria and BG-11 (pH 7.4) freshwater media for algae. Bacterial enrichment was attempted aerobically at 37ºC, while the algae enrichment was at 30ºC with high light intensity. Under these enrichment conditions, no viable bacteria or algal species were recovered after 1 week of incubation for bacteria and 3 weeks incubation for algae. Since the fungus was the most prominently visible organism via photomicrography and the only organism recovered, the identification study focused on the fungal species.

The fungal DNA was sequenced from the ITS region, and a Basic Local Assignment Search Tool (BLAST) analysis was performed to compare nucleotide sequences that were identified to biological sequence

databases (National Center for Biotechnology Information). BLAST analysis revealed the fungal isolate was 100% identical to numerous species from the *Alternaria* genus of ascomycetous fungi.

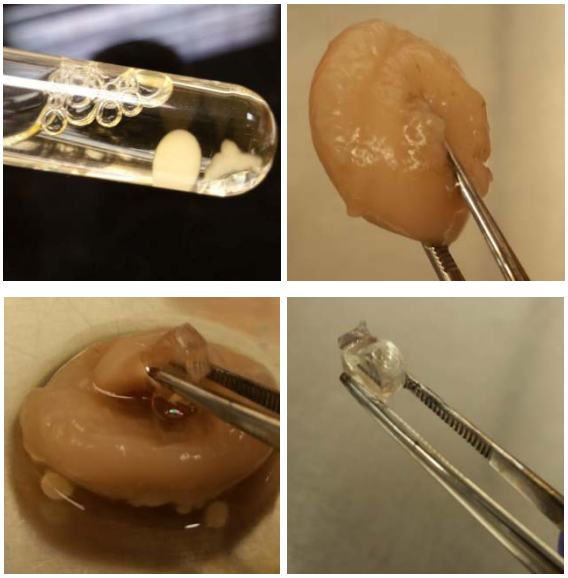

Figure 7: Images of fungal cultivation directly from glass shards obtained from a field-aged module (Argenbühl, Germany). Initial cultivation clearly showed a fungal mass adhered to the glass shard as well as a detached spherical fungal pellet (top left). Following transfer to a larger culture the attached fungus was able to completely encapsulate the glass shard (top right). The glass shard was then extracted (bottom left and bottom right) and used for DNA sequencing analysis.

3.2 Microscopy, profilometry, goniometry, and cleaning

Optical images of the dry-brushed and wet-sponged-squeegeed coated coupons of type A, B, D, E, and G showed mostly parallel striations or scratch patterns, whereas only limited to no scratching was found on the uncoated glass types J, T, and K under the same cleaning treatments. Dry-brush cleaning consistently showed more scratching than wet-sponge-squeegee cleaning for coated coupons, as can be seen by representative comparative images for coupon type E shown in Figure 8. The PMMA or plastic coupon showed more scratching than any of the coated glass specimens (Figure 9). None of the coupons (coated or uncoated) cleaned with the non-tactile methods (no-clean and water-spray) showed scratching.

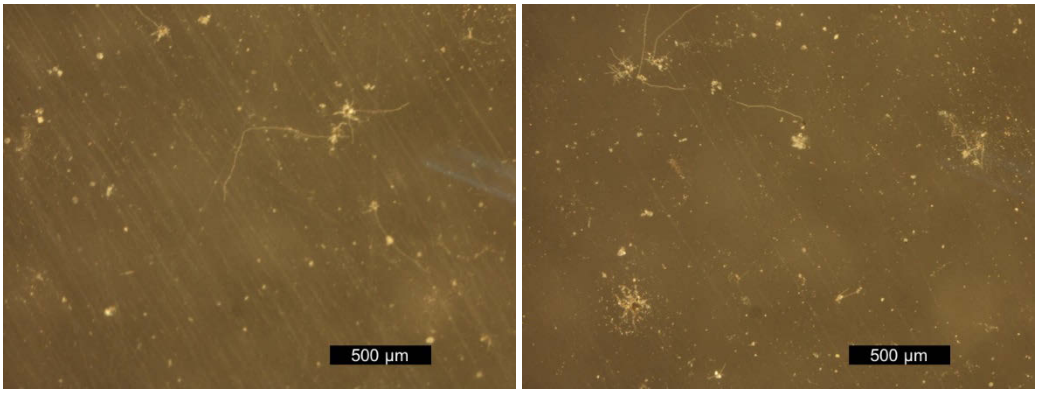

Figure 8. The coating of coupon E shows parallel scractch patterns that are generally representative for the coated specimens. Dry-brush cleaning (left) generally shows more scratches than wet-sponge-squeegee cleaning (right). Coupons shown have been rinsed.

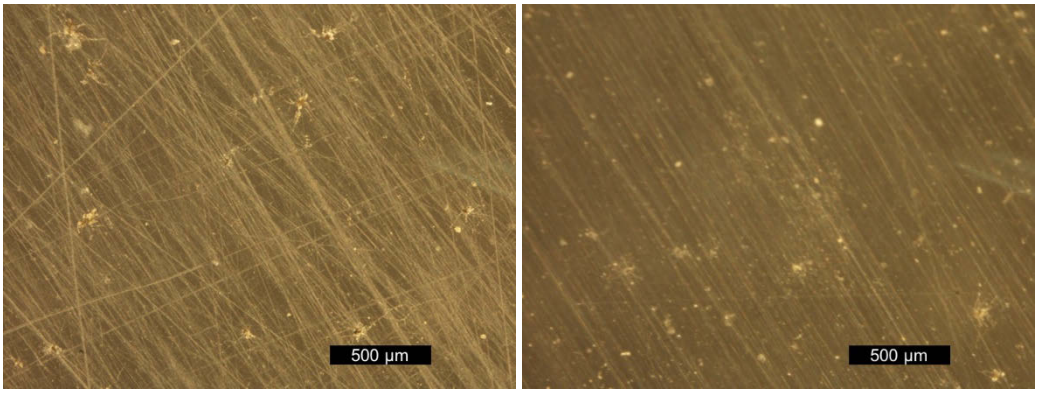

Figure 9: Microscope images of the A (PMMA) coupons; dry-brushed (left) and wet-sponge-squeegeed (right). PMMA shows more scratches than any of the coated glass specimens. The dry-brush on PMMA is the only case where oblique scratches are observed in addition to the parallel scratch patterns seen in other coupons. Coupons shown have been rinsed.

Average surface roughness measurements revealed features ranging from 4 to 30 nm across rinsed and wiped tempered coupons; the baseline, never deployed in the field and measured in the wiped state, is shown on the far right for comparison (Figure 10). Surface roughness for the rinsed coupons is almost an order of magnitude higher than for the wiped coupons due to the remaining stuck-on soiling. On average, roughness levels are highest for the no-clean and water-spray rinsed coupons, which were the non-tactile cleaning methods. Additionally, the slight increase in roughness even on the wiped coupons as compared to the baseline suggests that either some contamination was not removed or the underlying glass has been permanently roughened due to weathering.

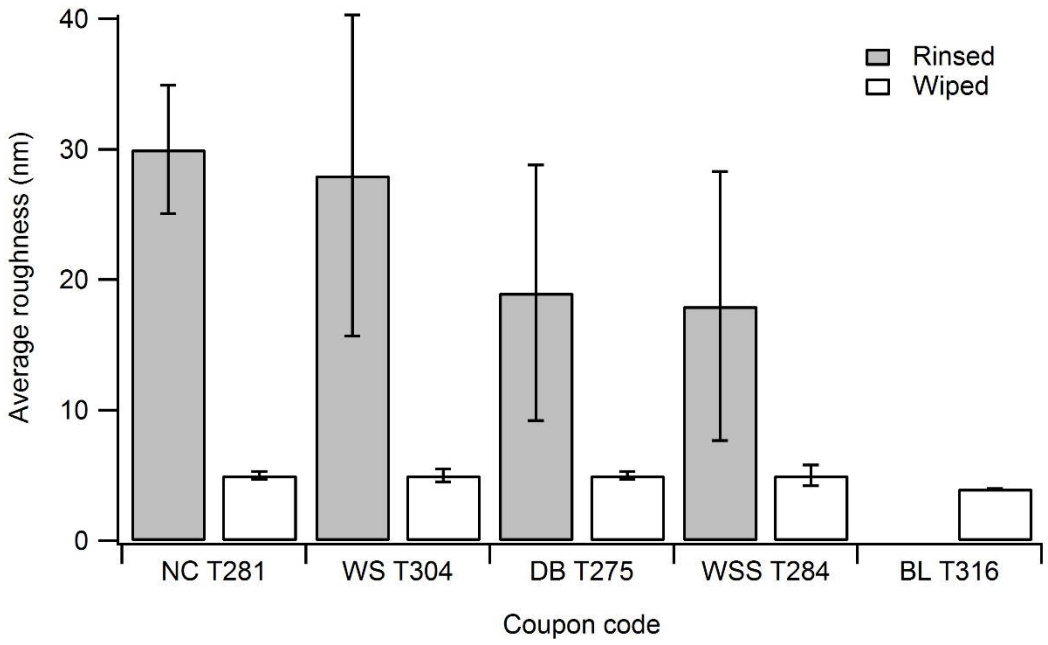

Figure 10: Average surface roughness of T coupons per each of the field cleaning methods after both rinsing and wiping. Error bars represent two standard deviations; each result represents the average of three measurements. In the coupon code, the cleaning practices are abbreviated as NC (no-clean), DB (dry-brush), WS (water-spray), or WSS (wet-sponge-squeegee), and compared to the baseline abbreviated as BL.

Even after the 1-minute wiping process, some contamination remains on the coupon surface. Figure 11 shows optical profilometer images for rinsed (left) and wiped (right) tempered coupons.

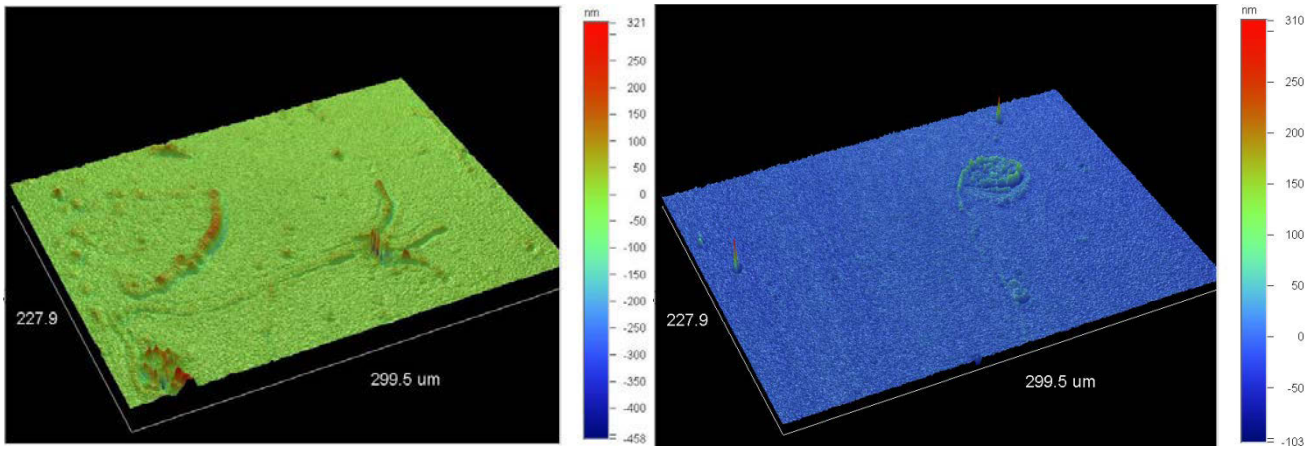

Figure 11: 3-D surface optical profilometry images of a rinsed (left) and wiped (right) water-sprayed T (tempered, uncoated) coupon.

Contact-angle measurements ranged from 17 to 66 degrees for rinsed tempered coupons as shown in Figure 12. DIW measurements show that the polar character of the aged coupons increases compared to the

baseline tempered coupon; diiodomethane and formamide measurements show relatively little change in the van der Waals and acid/base interactions. Changes in surface energy could result from the accumulation of surface contamination or changes in chemistry at the sample surface.

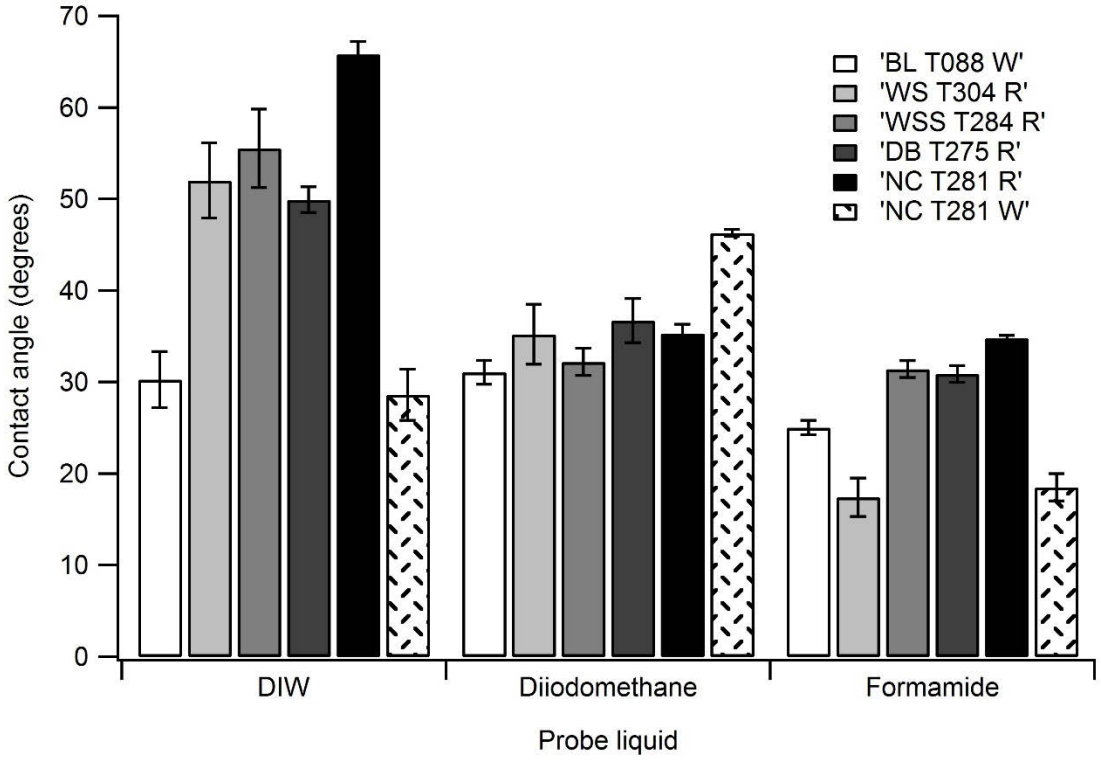

Figure 12: Contact angle of DIW, diiodomethane, and formamide on rinsed T (tempered) coupons. Error bars represent two standard deviations; each result represents the average of three measurements. In the coupon code, the cleaning practices are abbreviated as NC (no-clean), DB (dry-brush), WS (water-spray), or WSS (wet-sponge-squeegee), and compared to the baseline abbreviated as BL. Pre-measurement rinse and wipe are abbreviated as R and W, respectively.

In addition, micrographs of the no-clean and water-spray H coupons revealed unique surface features that were not present on the dry-brush and wet-sponge-squeegee H coupons (Figure 13). The inset in Figure 13 shows that the mottled surface texture (as well as fungal and particulate contamination) is completely removed by wiping. This suggests that the mottled texture is degraded coating material that remains weakly attached to the surface. It is expected that no texture is seen on the H coupons cleaned using mechanical contact because the coating was completely removed by cleaning.

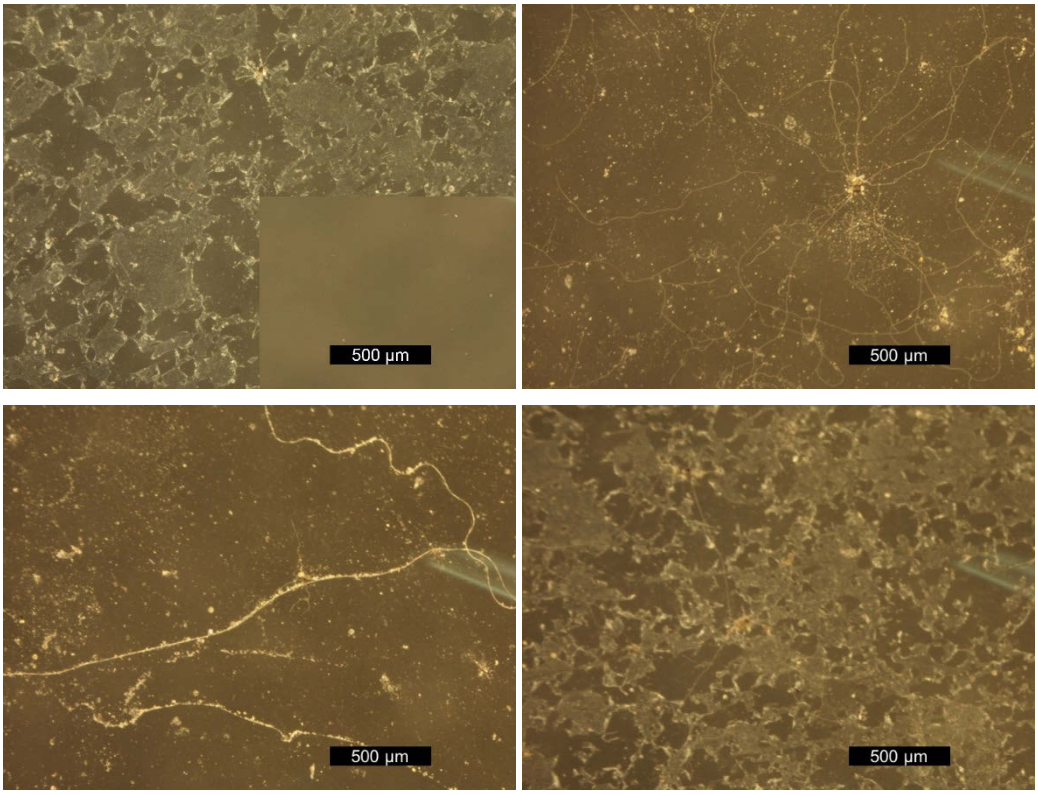

Figure 13: H coupon: no-clean (top left), no-clean and wiped (inset), wet-sponge-squeegee (top right), dry-brush (bottom left), and water-spray (bottom right). All micrographs other than the inset were rinsed.

3.3 Soiling and transmittance losses

Hemispherical transmittance measurements yielded no statistically significant differences between cleaning practices as shown in Figure 14; solar-weighted photon transmittance (SWT) was approximately 91.1% for the baseline tempered coupon. The no-clean T281 coupon was wiped and measured to quantify transmittance recovery, but this also varied within the range of instrument repeatability, on the order of +/- 0.6% [33]. The minimal loss (<1%) in hemispherical transmittance between the specimens in Figure 14 demonstrates that the mechanisms of optical reflection and absorption do not play a significant role for the coupon(s).

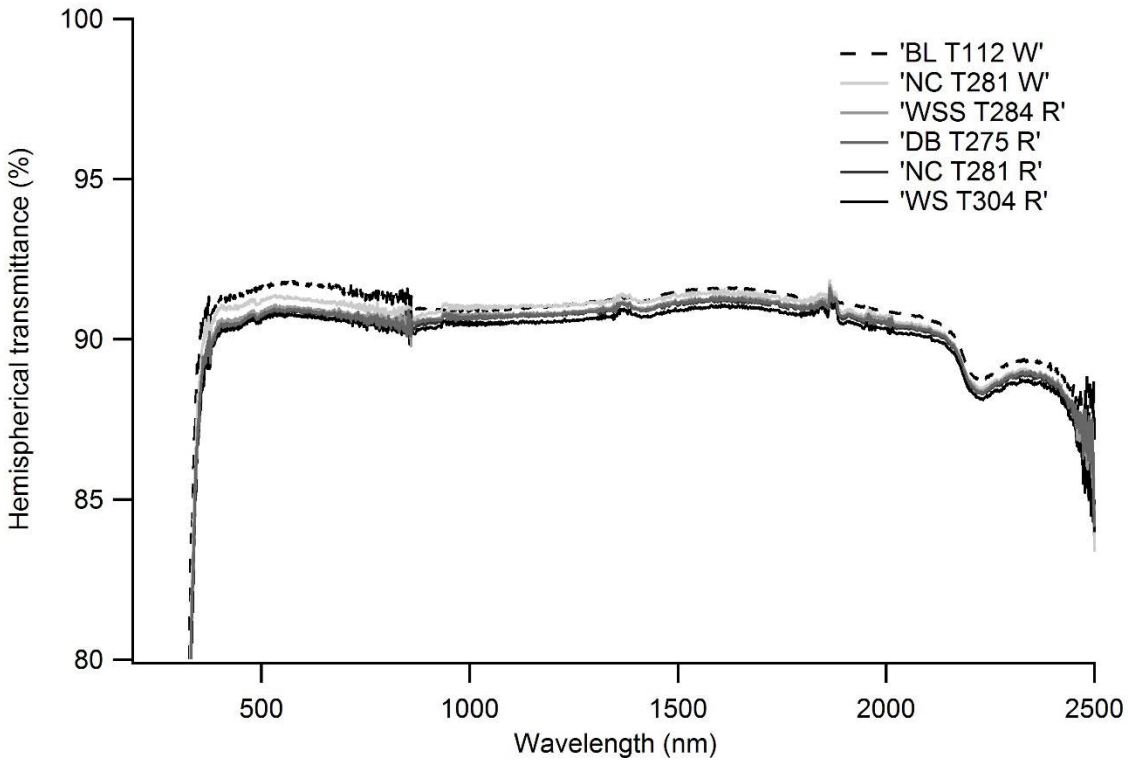

Figure 14: Hemispherical transmittance is shown for all field cleaning methods on the T coupons after the 5-second rinse. Results shown are averages of three measurements on the same coupon. In the coupon code, the cleaning practices are abbreviated as NC (no-clean), DB (dry-brush), WS (water-spray), or WSS (wet-sponge-squeegee), and compared to the baseline abbreviated as BL. Pre-measurement rinse and wipe are abbreviated as R and W, respectively.

As shown in Figure 15, direct transmittance measurements readily distinguish the cleaning methods applied to the fielded tempered coupons. SWT for the baseline coupon was approximately 91.9%. The no-clean tempered coupon that was wiped and re-measured followed closely at 91.4%, demonstrating the ability to almost fully restore transmittance to baseline levels. SWT was 88.4% for the dry-brush rinsed coupon, then 88.2% for the wet-sponge-squeegee rinsed coupon, then 87.3% for the no-clean rinsed coupon, then 87.0% for the water-spray rinsed coupon. By comparing to the hemispherical transmittance in Figure 14, the optical loss (approaching almost 5%) for the direct transmittance measurements in Figure 15 can be attributed to optical scattering. The comparison of hemispherical and direct transmittance fully clarifies that the dominant mode of optical degradation for the field-contaminated and -abraded glass specimens is forward scattering, not optical behavior related to absorption or reflection. Direct transmittance is most greatly reduced in Figure 15 at short wavelengths, i.e., optical haze [32] was found to vary with wavelength. A spurious spike in transmittance is observed in Figures 14, 15 and 16 at 860 nm, and is a result of the grating change for the instrument during scanning.

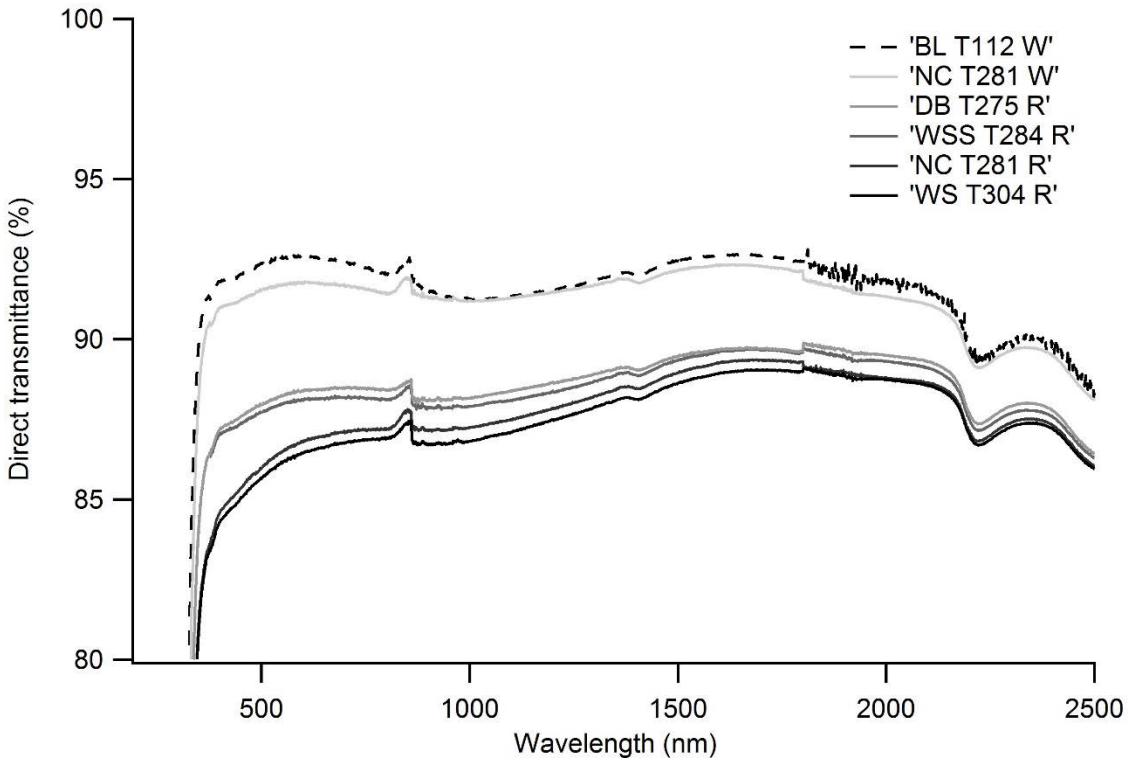

Figure 15: Direct transmittance is shown for all field cleaning methods for the T (tempered) coupons. Results shown are averages of three measurements on the same coupon. In the coupon code, the cleaning practices are abbreviated as NC (no-clean), DB (dry-brush), WS (water-spray), or WSS (wet-sponge-squeegee), and compared to the baseline abbreviated as BL. Pre-measurement rinse and wipe are abbreviated as R and W, respectively.

Figure 16 shows the direct transmittance measurements of a rinsed and then wiped no-clean H (AS-coated) coupon. There is a loss in direct transmittance due to soiling and/or coating damage that is recovered by wipe cleaning. This is consistent with the images in Figure 12, which suggest the wiping removes the damaged coating and any soiling. A minimal difference in optical performance is expected for the fielded H coupon cleaned by wiping because the coating primarily provides AS, not AR, functionality. The baseline measurement of an unaged H coupon was found to provide a SWT of 92.3%, an improvement in optical transmittance over that of the 91.7% for baseline uncoated Diamant (J) glass. Comparatively, the no-clean wiped H coupon provides a slightly lowered SWT of 91.3%, whereas the no-clean rinsed H coupon provides a SWT of 87.5%.

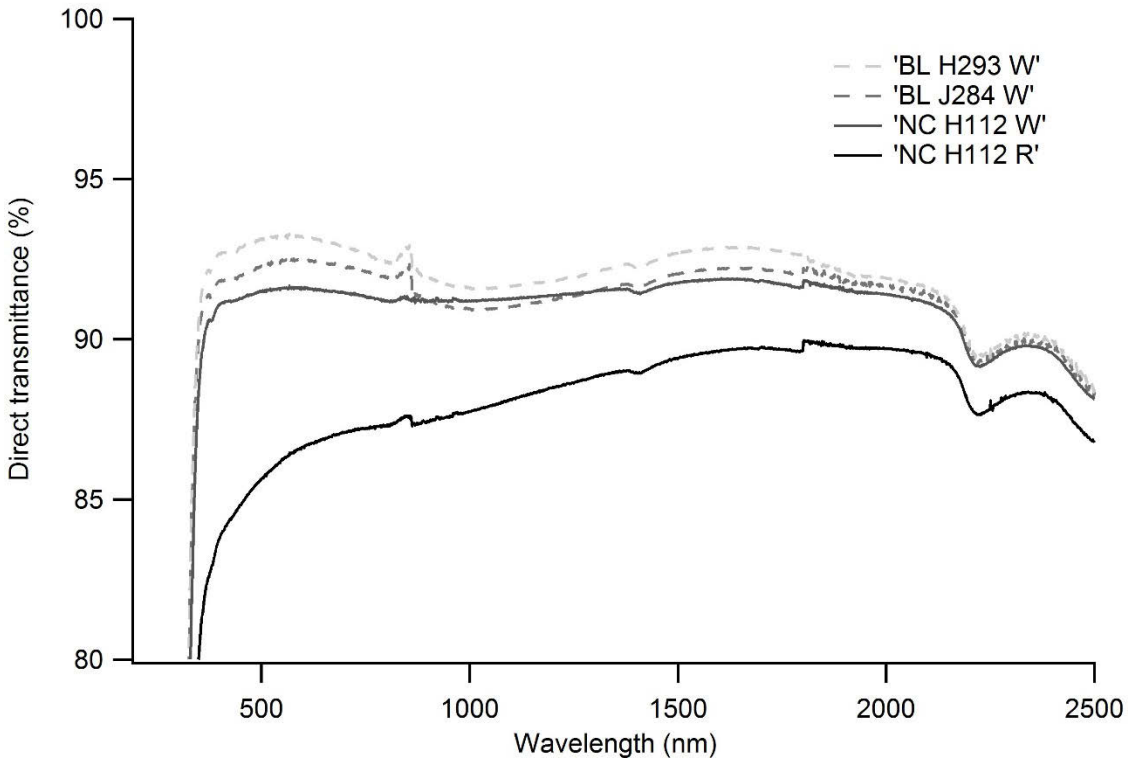

Figure 16: Direct transmittance of rinsed and wiped no-clean H (AS-coated) coupon. Unaged J (uncoated, untempered) and H coupons are shown for reference. The no-clean H coupon did not fully recover to its baseline measurement when wiped, indicating some of the coating may have been worn away. Results shown are averages of three measurements on the same coupon. In the coupon code, the cleaning practices are abbreviated as NC (no-clean), DB (dry-brush), WS (water-spray), or WSS (wet-sponge-squeegee), and compared to the baseline abbreviated as BL. Pre-measurement rinse and wipe are abbreviated as R and W, respectively.

3.4 Comparison to full-sized, field-aged module

Ongoing work evaluating full-sized, field-aged modules have found similar fungal contamination on modules from Argenbühl, Germany and Palms, California, as seen in Figure 17a,c,d. These fungal growths were comparable in appearance and texture to fungal growths observed on the glass coupons from Sacramento (Figure 17b). In both cases, long branching filamentous fungal structures (hyphae) were observed. Neither the rinse technique nor aggressively pressure-washing the surfaces with DIW for up to eight minutes removed the contamination effectively. The biofilm on the modules shown in Figure 17 were most effectively removed after the wiping technique. These initial findings suggest that PV modules in environments that subject to biological contamination may need to be cleaned more frequently. In addition, mild cleaning solutions may be required to effectively remove or limit the growth of fungal contaminants on PV modules.

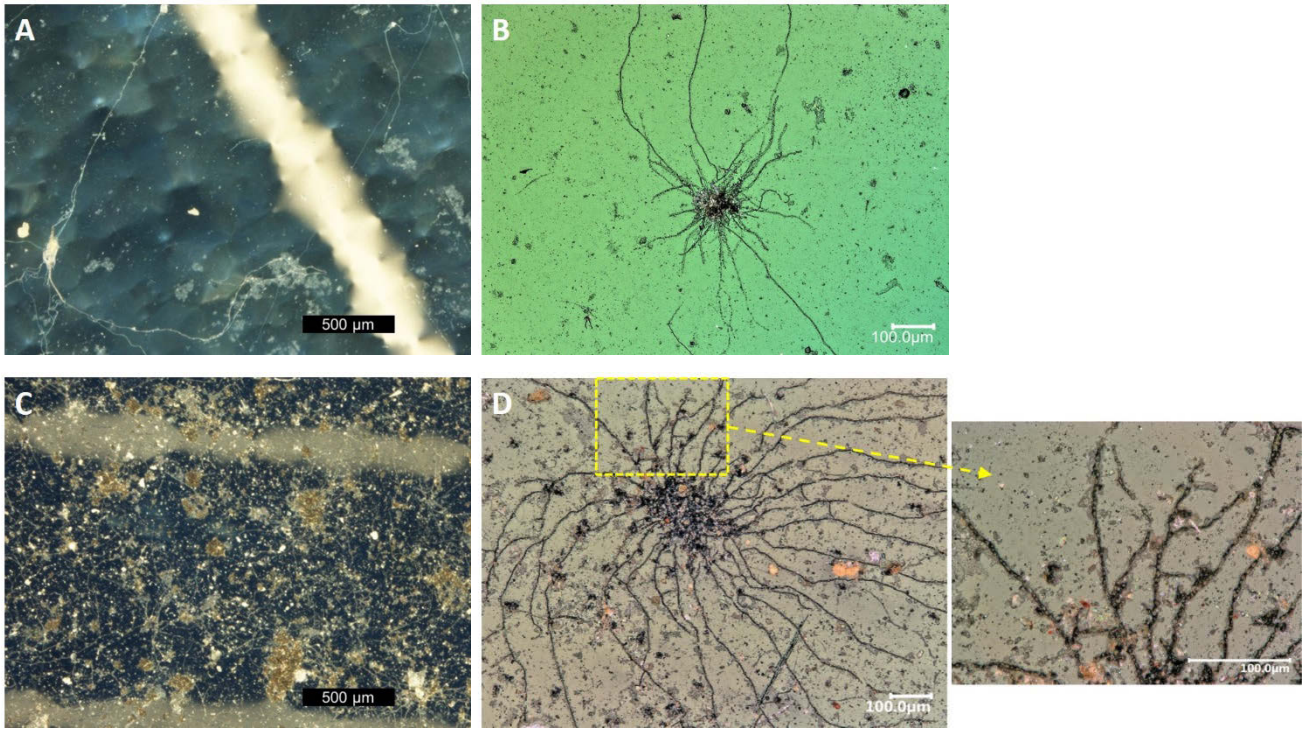

Figure 17: Micrographs of full-sized modules received after aging for 11 years in Palms, California (a), and 6 years in Argenbühl, Germany (c, d). The fungi on these modules are similar to the fungi found on the coupons in this study, such as NC J052 (b). Varying degrees of fungal contamination are seen on all surfaces, with the potential to severely reduce transmittance in more heavily soiled areas. White striations in the backgrounds of Figures 17a and 17c are bus bars under the module glass.

4. CONCLUSIONS

Although there are likely numerous biological species that may colonize PV modules, the main species found here is clearly capable of adhering to glass and is a member of the *Alternaria* genus. *Alternaria* species are widely distributed fungi that are primarily saprophytes that serve to decay organic matter [39]. The most likely route of contamination would be from deposition of spores in the ambient atmosphere. *Alternaria alternata* has been shown to possess a good ability to adhere to numerous surfaces [40]. Following the deposition of spores, the addition of moisture in the form of rainwater as well as energy and nutrients in the form of organic matter and carbon would facilitate spore germination and allow widespread colonization of the glass surface. The fungi were not found to have etched the glass in the specimens examined here. However, micrographs suggest that inorganic matter concentrates near and on the fungi. The biological contamination and its associated inorganic matter were not removed by the 5-second rinse, and in some cases fungi remained after a 1-minute wipe. Biological contamination is an example of soiling that cannot be removed by natural cleaning, i.e., 100% recovery of optical loss is not possible, as described in Ref. [20]. Fungal growths have previously been found on PV installations in the rain-prone climate of Sao Paulo, Brazil [17]. Considering that Sacramento is a drier climate, biofilms may play a more widespread role in PV soiling than previously realized. Hard-to-remove biofilms would fit into the

category of contamination called “cementation,” [41] because it takes a mechanical force such as a 1-minute wipe to remove the film.

A primary aspect of this 5-year experiment—deploying coated coupons in five locations—is to gather degradation data due to weathering, natural abrasion, and abrasion from cleaning practices. It is clear from the optical images and roughness measurements that degradation has occurred for all coatings after one year of field weathering near Sacramento. In the worst case, the H coating appears to have been extensively damaged from the combination of weathering and mechanical-contact cleaning; it is difficult to claim whether other coatings remain, have degraded, or have been completely worn away. In the case of all other coatings, scratches are present in highest quantity for dry-brush cleaning, but are also present for wet-sponge-squeegee cleaning. In contrast, scratches are not present when only water-spray cleaning or no-cleaning is used. The coated glass specimens show less scratch abrasion than PMMA. While the initial results here are limited, methods to more quantitatively distinguish between the cleaning methods and identify the relative durability of the coatings (including high dynamic range optical microscopy and software image analysis) are being developed. The difficulties are that the coatings may not be homogenously removed within the entire region of examination, and the effect of remaining contamination cannot be readily decoupled. Future work will include developing methods to assess the integrity of the coatings relative to baseline electron-microscopy and other characterizations.

The losses accrued here after one year could contribute to the degradation in performance through 25-year product life of a PV module. Comparing hemispherical and direct transmittance measurements suggests that the dominant mode of optical degradation for the field-contaminated and -abraded glass specimens is forward scattering, not absorption or reflection. The effects of abrasion are therefore likely to have a minor effect (i.e. not exceeding the angle of acceptance) for the specimens examined here. Soiling and related abrasion in this case occur after only one year in the field in a location that was expected to have a low soiling rate relative to the other locations in this study. It is possible that more frequent or aggressive cleaning could reduce soiling. However, monthly cleanings were used in this study because it is difficult to rely on remote operators to maintain a more frequent cleaning schedule. Interestingly, the water-spray cleaning method resulted in the largest losses in transmittance (even more than the no-clean method), and the dry-brush cleaning method resulted in the least losses in transmittance; it is possible that the increased presence of water on the surface of the coupons due to water-spray cleaning could affect the chemical composition of inorganic species and/or the biological colonization of the glass surface. None of the cleaning methods or coatings in this study entirely prevented the accumulation of fungal growths and inorganic contamination. The wiping procedure (W) restored transmittance to near the baseline levels.

There exists a body of research on the applications of certain algicidal agents to roofing materials to prevent the growth of biological entities [38] [42] [43]. It is possible that similar methods can be applied for solar PV glass to reduce the accumulation of biological species. Considering the mixture of inorganic and organic contamination observed here, different cleaning methods may be required based on different climates. It has previously been shown that fungal growths on optical components can be removed using SC-1, a 50/50 mix of

hydrogen peroxide and ammonia [44]. The use of this cleaning method removed most, but not all, of coupon surface contamination; however, SC-1 is not a cleaning technique that could feasibly be used on full-sized modules in the field. More research is needed on low-cost, environmentally sustainable, and gentle cleansers or cleaning methods for PV glass.

5. ACKNOWLEDGEMENTS

This work was executed by the U.S. Department of Energy under Contract No. DE-AC36-08-GO28308 with Alliance for Sustainable Energy, LLC, the Manager and Operator of the National Renewable Energy Laboratory. Funding provided by U.S. Department of Energy Office of Energy Efficiency and Renewable Energy (EERE) under Solar Energy Technologies Office (SETO) Agreement Number 30311."

The authors would like to thank Greg Perrin (NREL), Byron McDanold (NREL), Dr. Craig Perkins (NREL), Michael Anderson (SunPower Corporation), and George Kelly (BP Solar) for their contributions. There are no competing interests.

6. REFERENCES

[1] H. Nancy, "Terawatt-scale photovoltaics: Trajectories and challenges," *Science,* 2017.

[2] International Energy Agency - PVPS, "Review of failures of photovoltaic modules," 2014.

[3] M. Leonardo and M. Muller, "An Investigation of the Key Parameters for Predicting PV Soiling Losses," *Progress in Photovoltaics: Research Applications,* no. 25, pp. 291-307, 2017.

[4] A. Kimber, L. Mitchell, S. Nogradi and H. Wenger, "The effect of soiling on large grid-connected photovoltaic systems in California and the southwest region of the United States," *Photovoltaic Energy Conversion,* Conference Record of the 2006 IEEE 4th World Conference, 2006.

[5] S. Canada, "Impacts of soiling on utility-scale PV system performance," *SolarPro Magazine,* 2016.

[6] J. R. Caron and B. Littmann, "Direct Monitoring of energy lost due to soiling on first solar modules in California," *IEEE Journal of Photovoltaics,* vol. 3, no. 1, pp. 336-340, 2013.

[7] F. A. Mejia and J. Kleissl, "Soiling losses for solar photovoltaic systems in California," *Solar Energy,* no. 95, pp. 357-363, 2013.

[8] B. Guo, W. Javed, B. W. Figgis and T. Mirza, "Effect of dust and weather conditions on photovoltaic performance in Doha, Qatar," *1st Workshop on Smart Grid and Renewable Energy,* 2015.

[9] H. J. Möller and H. A. AlBusair, "Performance evaluation of CdTe PV modules under natural outdoor conditions in Kuwait," *EU PVSEC 25; 10,* 2010.

[10] R. K. Jones, A. Baras, A. Al Saeeri, A. Al Qahtani, A. O. Al Amoudi, Y. Al Shaya and et al, "Optimized cleaning cost and schedule based on observed soiling conditions for photovoltaic plants in central Saudi Arabia," *IEEE Journal of Photovoltaics,* vol. 6, no. 3, pp. 730-738, 2016.

[11] A. Salim, F. Huraib and N. Eugenio, "PV power-study of system options and optimization," *Proceedings of the 8th European PV Solar Energy Conference,* 1988.

[12] U. Rahoma, A. Hassan, H. Elminir and A. Fathy, "Effect of airborne dust concentration on the performance of PV modules," *Journal of Astronomical Society Egypt,* vol. 13, no. 1, pp. 24-38, 2005.

[13] B. Nimmo and S. Saed, "Effects of dust on the performance of thermal and photovoltaic flat plat collectors in Saudi Arabia: Preliminary results," *Alternative Energy Sources,* vol. 2, pp. 145-152, 1979.

[14] National Renewable Energy Laboratory, "Photovoltaic modules soiling map," 2018. [Online]. Available: www.nrel.gov/pv/soiling.html.

[15] S. C. S. Costa, A. S. A. C. Diniz and L. L. Kazmerski, "Dust and soiling issues and impacts relating to solar energy systems: Literature review update for 2012–2015," *Renewable and Sustainable Energy Reviews,* vol. 63, pp. 33-61, 2016.

[16] A. Hoffman and J. Griffith, "Environmental Testing of Terrestrial Flat Plate Photovoltaic Modules," *In Proc. 14th Intersociety Energy Conversion Engineering Conference,* vol. 1, pp. 230-238, NASA JPL, CALTECH 1979.

[17] M. Shirakawa, R. Zilles, A. Mocelin, C. Gaylarde, A. Gorbushina, G. Heidrich, M. Giudice, G. Gilda Del Negro and V. John, "Microbial colonization affects the efficiency of photovoltaic panels in a tropical environment," *Journal of Environmental Management,* vol. 157, pp. 160-167, 2015.

[18] S. Noack-Schönmann, O. Spagin, K. P. Gründer, M. Breithaupt, A. Günter, B. Muschik and A. Gorbushina, "Sub-aerial biofilms as blockers of solar radiation: spectral properties as tools to characterise material relevant microbial growth," *International Biodeterioration & Biodegradation,* vol. 86, pp. 286-293, 2014.

[19] A. Gorbushina, "Life on the rocks," *Environmental Microbiology,* vol. 9, no. 7, pp. 1613-1631, 2007.

[20] T. Sarver, A. Qaraghuli and L. Kazmerski, "A comprehensive review of the impact of dust on the use of solar energy: History, investigations, results, literature, and mitigation approaches," *Renewable and Sustainable Energy Reviews,* vol. 22, pp. 698-733, 2013.

[21] D. Miller, M. Muller and L. Simpson, "Review of Artificial Abrasion Test Methods for PV Module Technology," No. NREL/TP-5J00-66334, National Renewable Energy Laboratory (NREL), Golden, CO (United States), 2016.

[22] Z. Abrams, P. Gonsalves, B. Brophy and J. Posbic, "Field And Lab Verification of Hydrophobic Ant-reflective and Anti-soiling coatings on Photovoltaic Glass," *Proceedings of the 29th PVSEC,* 2013.

[23] C. Cañete, R. Moreno, J. Carretero, M. Piliougine, M. Sidrach-de-Cardona, J. Hirose and S. Ogawa, "Effect Of The Self-Cleaning Coating Surface In The Temperature And Soiling Losses Of Photovoltaic Modules," *Proceedings of the 27th PVSEC,* 2011.

[24] E. Klimm, T. Lorenz and K. A. Weiss, "Can Anti-Soiling Coating on Solar Glass Influence the Degree of Performance Loss Over Time of PV Modules Drastically?," *Proceedings of the 28th PVSEC,* 2012.

[25] K. Midtdal and B. P. Jelle, "Self-Cleaning Glazing Products: A State-of-the-Art Review and Future Research Pathways," *Solar Energy Materials & Solar Cells,* vol. 109, pp. 126-141, 2013.

[26] M. C. Peel, B. L. Finlayson and T. A. McMahon, "Updated world map of the Köppen-Geiger climate classification," *Hydrology and earth system sciences discussions,* vol. 4, no. 2, pp. 439-473, 2007.

[27] A. M. Al-Dousari, "Dust phenomena, Kuwait case study," *International workshop on sand and dust storms,* 2016.

[28] A. A. Al-Kulaib, in *Climate of Arabian Gulf*, Kuwait, That Alsalasil Press, p. 87.

[29] A. van Donkelaar, R. V. Martin, M. Brauer, N. C. Hsu, R. A. Kahn, R. C. Levy, A. Lyapustin, A. M. Sayer and D. M. Winker, "Global Estimates of Fine Particulate Matter using a Combined

Geophysical-Statistical Method with Information from Satellites, Models, and Monitors," *Environ. Sci. Technol,* 2016.

[30] H. K. Raut and V. A. Ganesh, "Anti-reflective coatings: A critical, in-depth review," *Energy Environ. Sci.,* vol. 4, pp. 3779-3804, 2011.

[31] D. C. Miller, "An End of Service Life Assessment of PMMA Lenses from Veteran Concentrator Photovoltaic Systems," *SOLMAT,* vol. 167, pp. 7-21, 2017.

[32] IEC 62788-1-4, "Measurement procedures for materials used in photovoltaic modules - Part 1-4: Encapsulants - Measurement of optical transmittance and calculation of the solar-weighted photon transmittance, yellowness index, and UV cut-off wavelength," *International Electrotechnical Commission: Geneva,* pp. 1-37, 2016.

[33] D. C. Miller, J. Apezteguia, J. G. Bokria, M. Köhl, N. E. Powell, M. E. Smith, M. D. White, H. R. Wilson and J. H. Wohlgemuth, "Examination of An Optical Transmittance Test for Photovoltaic Encapsulation Materials," *Proc SPIE,* pp. 8825-8, 2013.

[34] U. Drewello, "Biogenic surface layers on historical window glass and the effect of excimer laser cleaning," *J. Cult. Herit.,* vol. 1, 2000.

[35] G. Piñar, "Microscopic, chemical, and molecular-biological investigation of the decayed medieval stained window glasses of two Catalonian churches.," *Int. Biodeter. Biodeg.,* vol. 84, 2013.

[36] E. Mellor, "The decay of window glass from the point of view of the lichenous growth," *J. Soc. Glass Technol,* vol. 8, pp. 182-186, 1924.

[37] S. Rölleke, "Analysis of bacterial communities on historical glass by denaturing gradient gel electrophoresis of PCR-amplified gene fragments coding for 16S rRNA," *J. Microbiol. Methods,* vol. 36, pp. 107-114, 1999.

[38] L. Verhoef, The Soiling and Cleaning of Building Facades., London: Routledge, 1988.

[39] B. Thomma, "Alternaria spp.: from general saprophyte to specific parasite.," *Molecular plant pathology,* vol. 4.4, pp. 255-236, 2003.

[40] K. Ikeda, "The role of the extracellular matrix (ECM) in phytopathogenic fungi: a potential target for disease control.," *Plant Pathology,* 2012.

[41] H. R. Moutinho, "Adhesion mechanisms on solar glass: Effects of relative humidity, surface roughness, and particle shape and size," *Solar Energy Materials and Solar Cells,* vol. 172, pp. 145-153, 2017.

[42] W. S. Bigham, C. Sobon and B. L. George, "Tin-Acrylate-Containing Polymers As Algicidal Agents in building Materials". US Patent 5427793, 1995.

[43] P. Berdahl, "Weathering of roofing materials – An overview," *Construction and Building Materials,* vol. 22, pp. 423-433, 2008.

[44] I. Cordero, "Fungus: how to prevent growth and remove it from optical components," *Community Eye Health Journal: Equipment Care and Maintenance,* 2013.

7. APPENDIX

Figures:

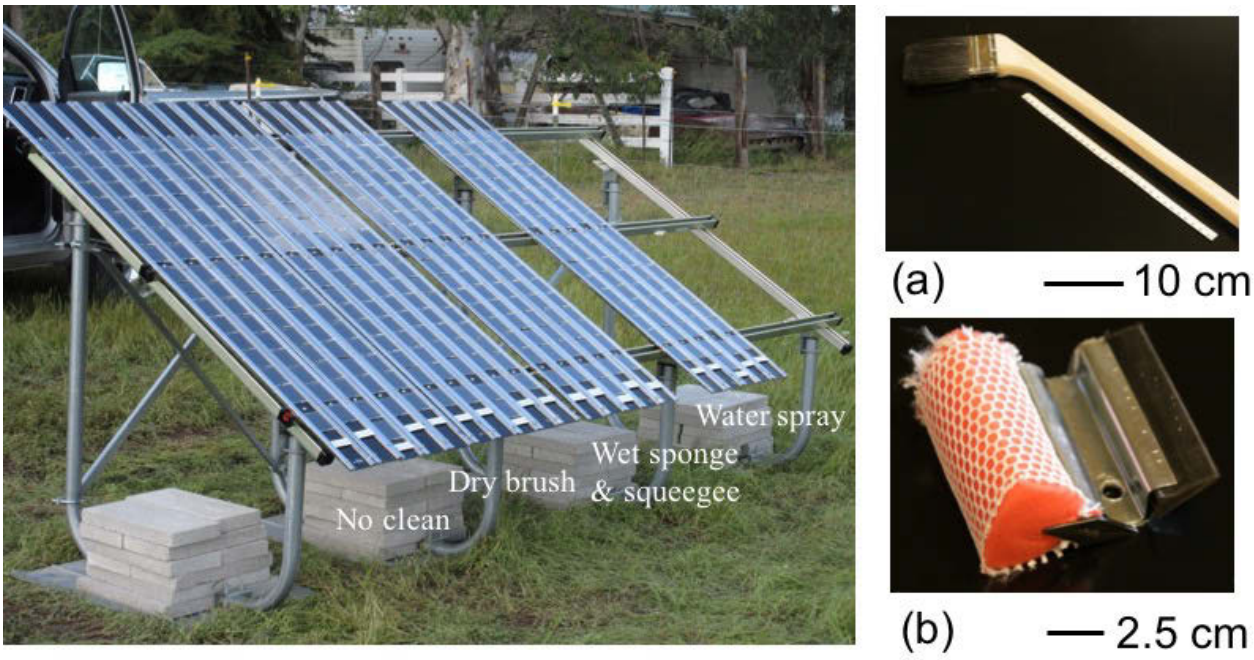

Figure 1: A 30-degree tilt rack with 20 coupon holders (each holding seventeen 75 mm × 75 mm coupons) as deployed outside Sacramento, California in April 2016. From left to right, the first coupon holders are never cleaned; the coupons in the next five holders are dry brushed monthly, the next five are rubbed with a wet sponge followed by a squeegee monthly, and the last five are water sprayed monthly. One coupon holder is removed from each set of cleaning methods each year and returned to NREL for each of the 5 years in the study. Figure 1 (a) shows a representative brush (with horse hair bristles) used for dry brush cleaning; Figure 1 (b) shows a representative head for a squeegee used with water.

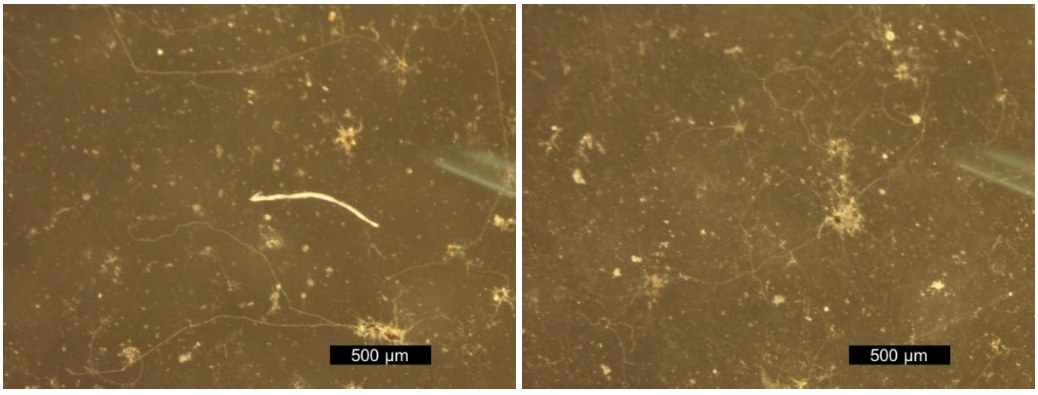

Figure 2: Micrograph of a water-sprayed T coupon (Diamant baseline tempered glass with no coating), as-received (left) and rinsed (right), showing particulates and the root-like filaments of the fungi. Most of the particulate matter and soiling as well as fungi remain after the 5-second rinse. Background tint results from the

microscope stage, and the chromatic artifact in the right of each image is a reflection of the ambient fluorescent lighting.

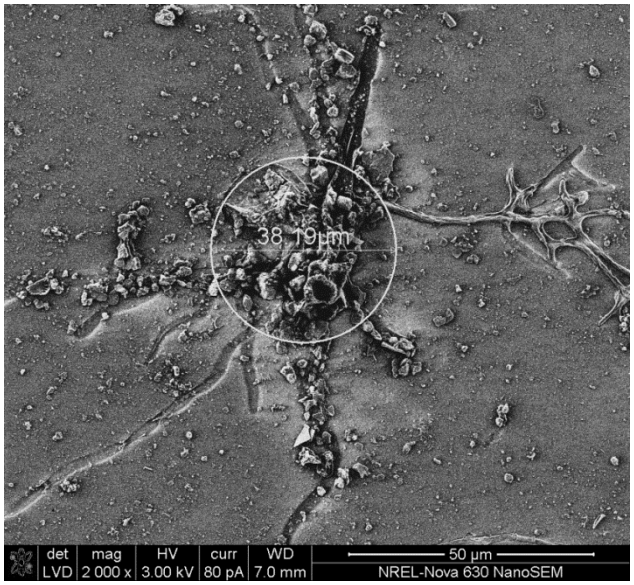

Figure 3: SEM image from the same coupon shown in Figure 2. The fungi centroid spans about 38 µm in diameter.

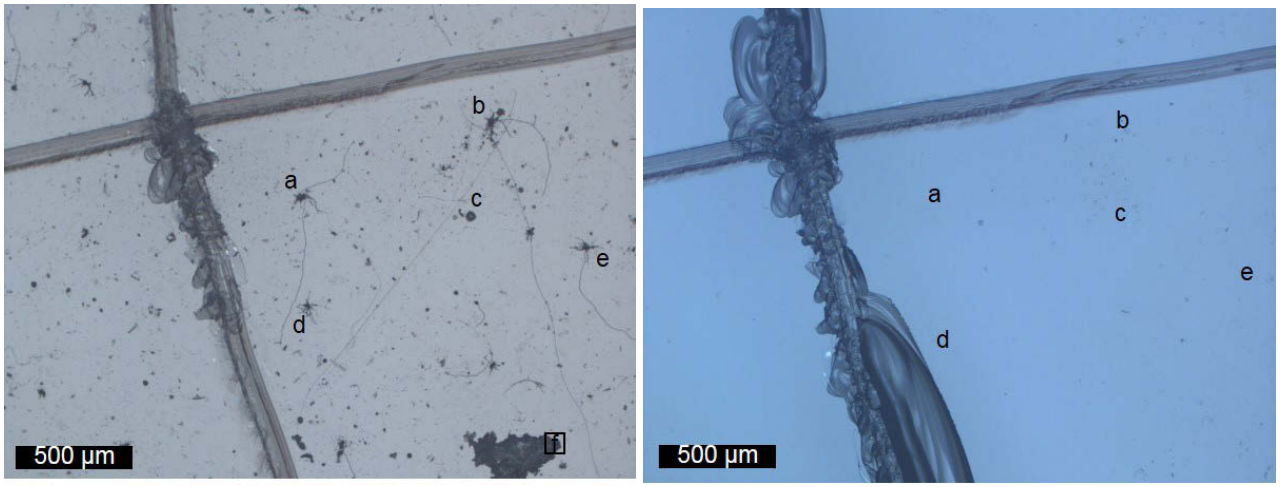

Figure 4: An optical image with indication of the locations of various fungi before (left) and after (right) the cleaning of coupon NC K198. The fungi at locations a–d have been removed, while only minor surface contamination remains on the specimen. Note that at location d the scribe is itself affected by cleaning. Differences in the cross used to mark the location of examination are attributed to the sonication during the cleaning process.

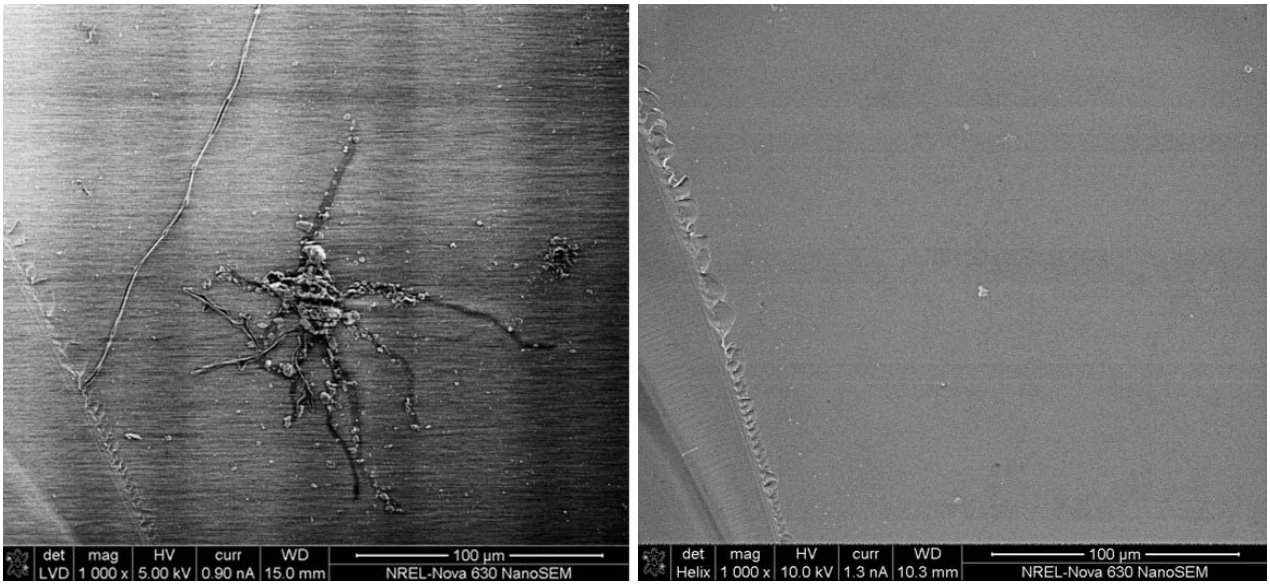

Figure 5: SEM images of location d in Figure 4 before (left) and after (right) cleaning with SC-1.

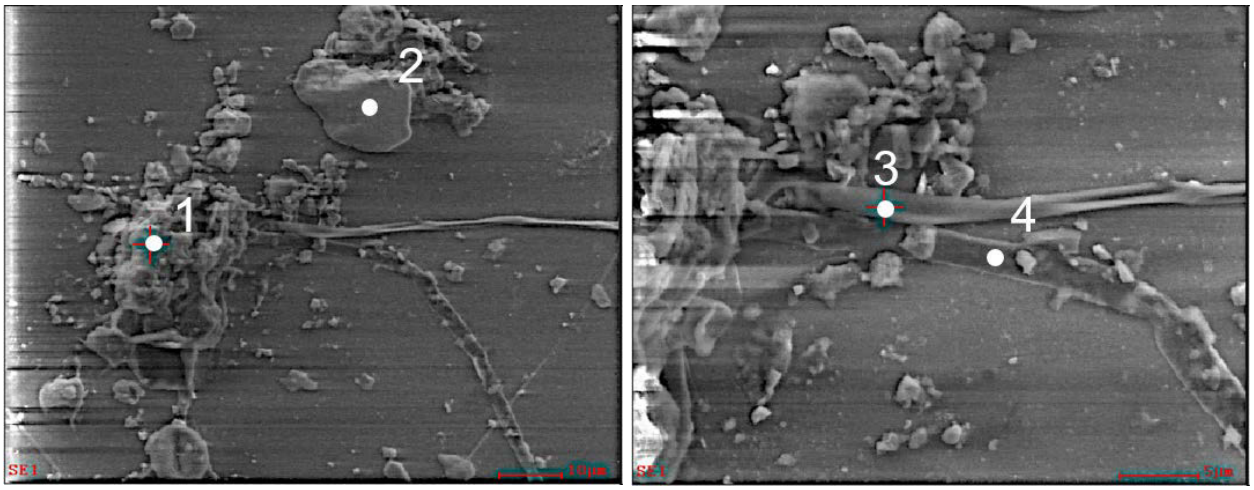

Figure 6: Specific SEM images from location b in Figure 4. Numbered locations on these SEM images were subject to EDS elemental composition analysis; results shown in Table 3.

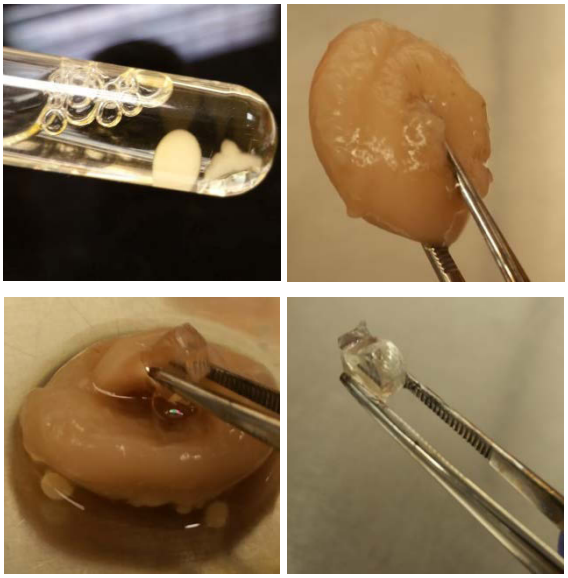

Figure 7: Images of fungal cultivation directly from glass shards obtained from a field-aged module (Argenbühl, Germany). Initial cultivation clearly showed a fungal mass adhered to the glass shard as well as a detached spherical fungal pellet (top left). Following transfer to a larger culture the attached fungus was able to completely encapsulate the glass shard (top right). The glass shard was then extracted (bottom left and bottom right) and used for DNA sequencing analysis.

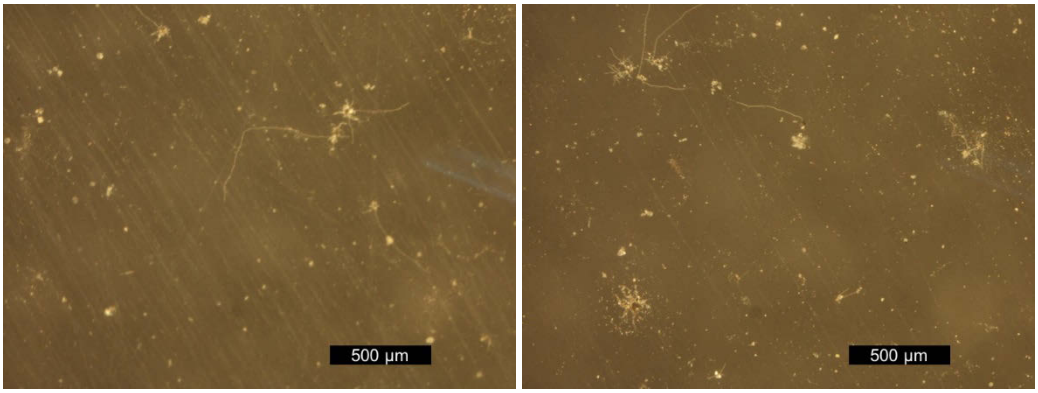

Figure 8. The coating of coupon E shows parallel scractch patterns that are generally representative for the coated specimens. Dry-brush cleaning (left) generally shows more scratches than wet-sponge-squeegee cleaning (right). Coupons shown have been rinsed.

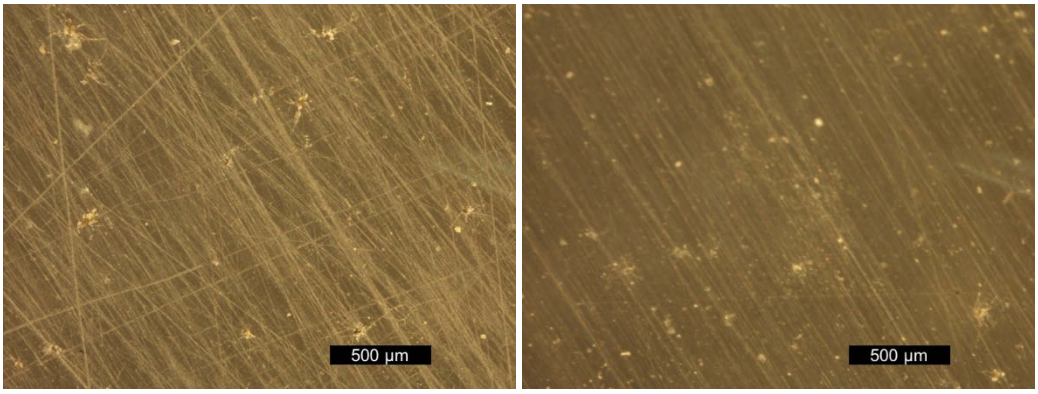

Figure 9: Microscope images of the A (PMMA) coupons; dry-brushed (left) and wet-sponge-squeegeed (right). PMMA shows more scratches than any of the coated glass specimens. The dry-brush on PMMA is the only case where oblique scratches are observed in addition to the parallel scratch patterns seen in other coupons. Coupons shown have been rinsed.

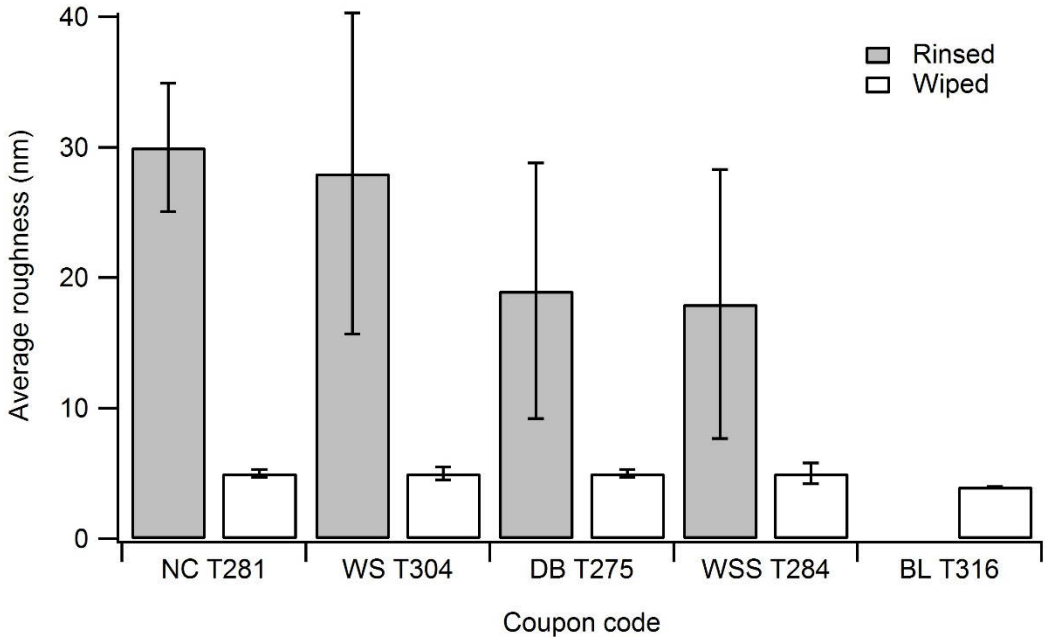

Figure 10: Average surface roughness of T coupons per each of the field cleaning methods after both rinsing and wiping. Error bars represent two standard deviations; each result represents the average of three measurements. In the coupon code, the cleaning practices are abbreviated as NC (no-clean), DB (dry-brush), WS (water-spray), or WSS (wet-sponge-squeegee), and compared to the baseline abbreviated as BL.

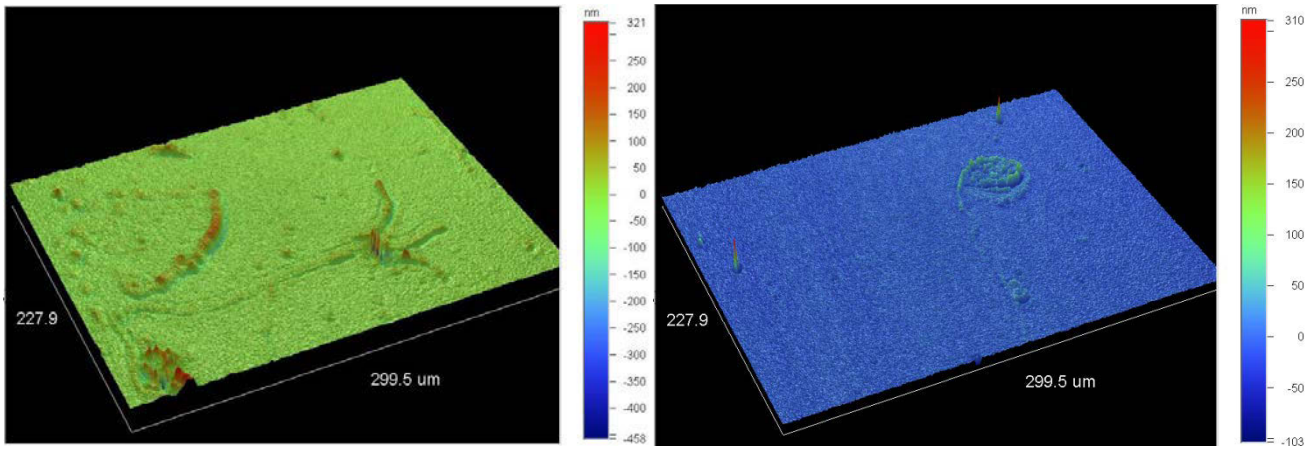

Figure 11: 3-D surface optical profilometry images of a rinsed (left) and wiped (right) water-sprayed T (tempered, uncoated) coupon.

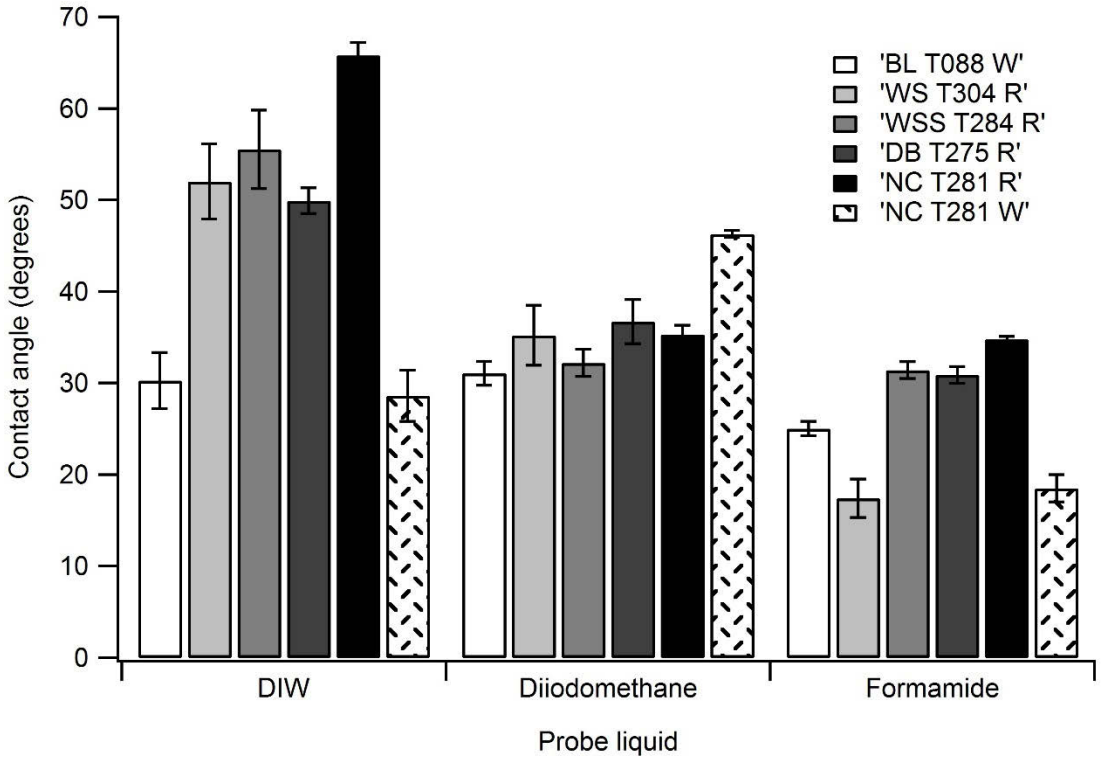

Figure 12: Contact angle of DIW, diiodomethane, and formamide on rinsed T (tempered) coupons. Error bars represent two standard deviations; each result represents the average of three measurements. In the coupon code, the cleaning practices are abbreviated as NC (no-clean), DB (dry-brush), WS (water-spray), or WSS (wet-sponge-squeegee), and compared to the baseline abbreviated as BL. Pre-measurement rinse and wipe are abbreviated as R and W, respectively.

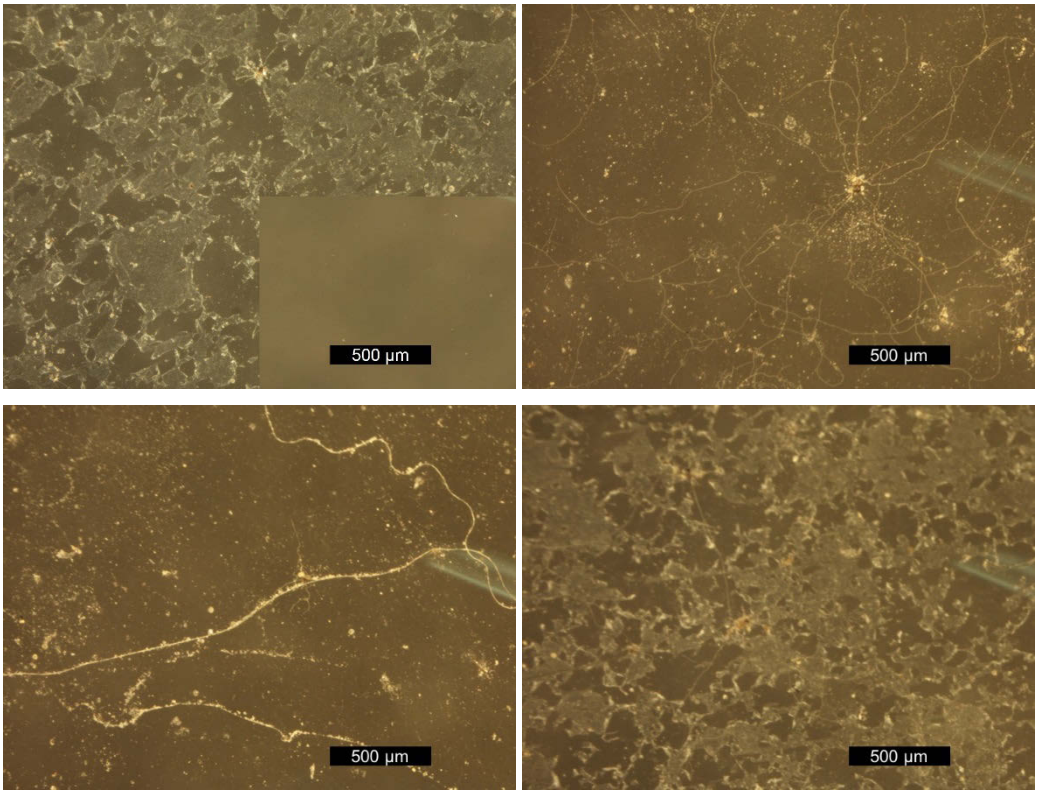

Figure 13: H coupon: no-clean (top left), no-clean and wiped (inset), wet-sponge-squeegee (top right), dry-brush (bottom left), and water-spray (bottom right). All micrographs other than the inset were rinsed.

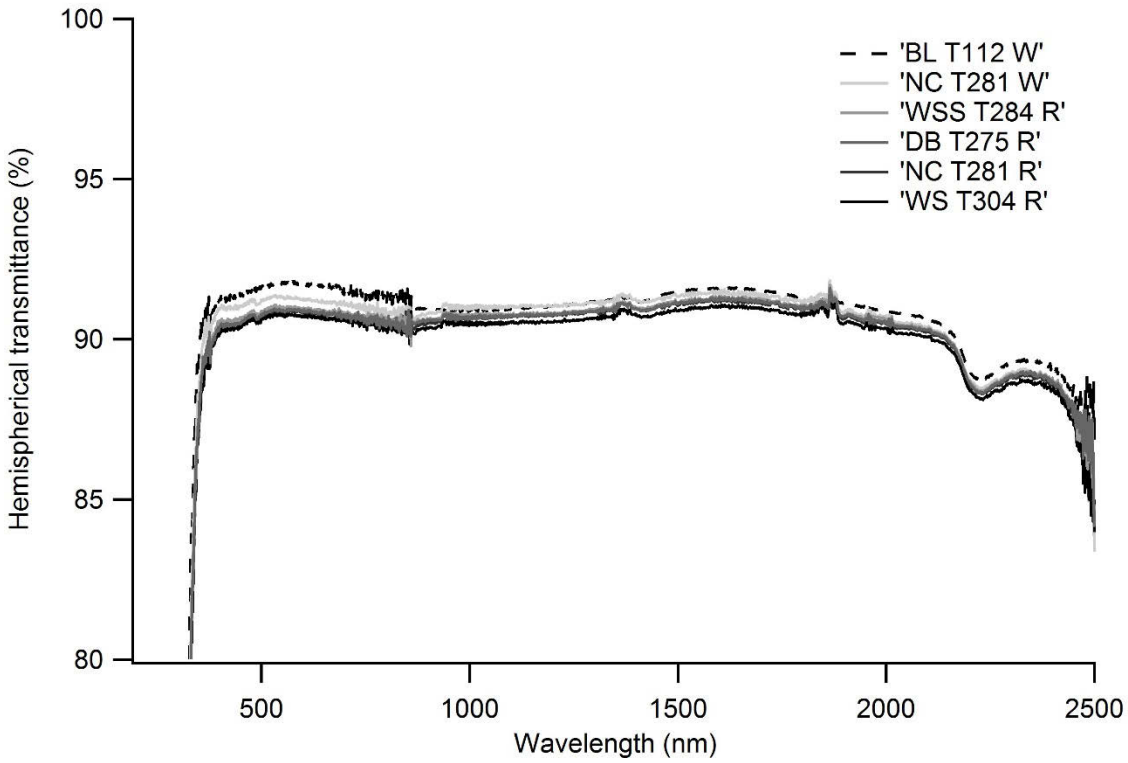

Figure 14: Hemispherical transmittance is shown for all field cleaning methods on the T coupons after the 5-second rinse. Results shown are averages of three measurements on the same coupon. In the coupon code, the cleaning practices are abbreviated as NC (no-clean), DB (dry-brush), WS (water-spray), or WSS (wet-sponge-squeegee), and compared to the baseline abbreviated as BL. Pre-measurement rinse and wipe are abbreviated as R and W, respectively.

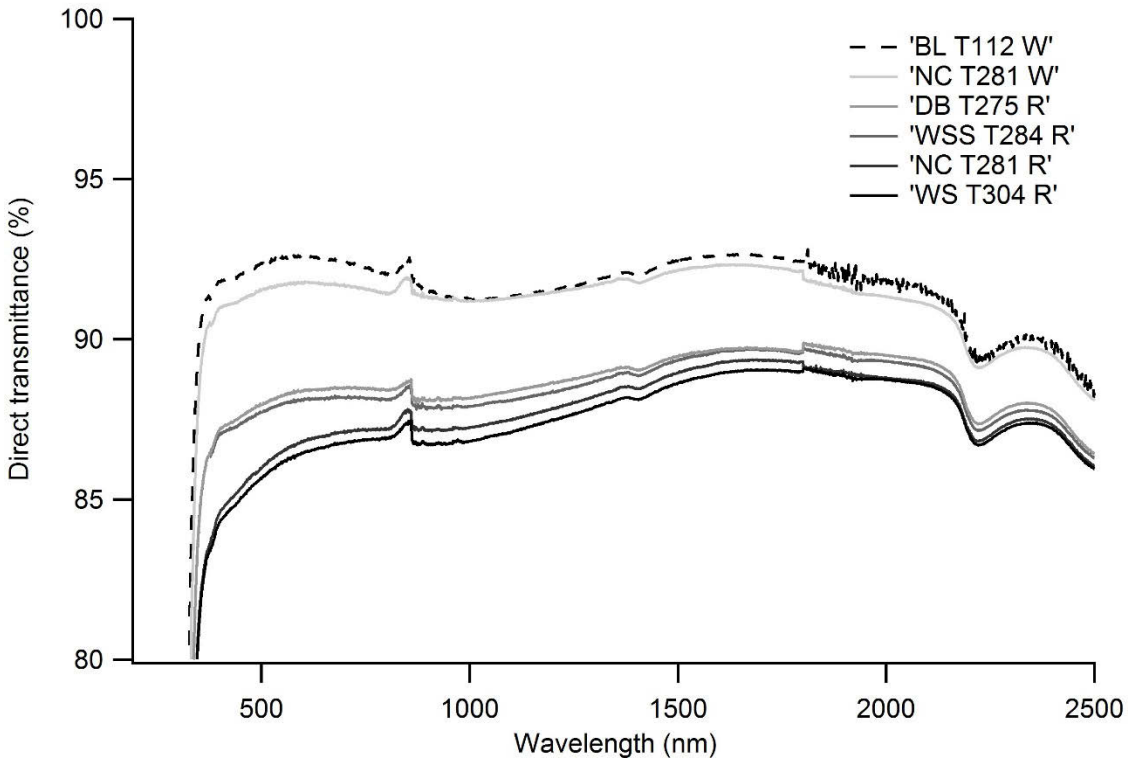

Figure 15: Direct transmittance is shown for all field cleaning methods for the T (tempered) coupons. Results shown are averages of three measurements on the same coupon. In the coupon code, the cleaning practices are abbreviated as NC (no-clean), DB (dry-brush), WS (water-spray), or WSS (wet-sponge-squeegee), and compared to the baseline abbreviated as BL. Pre-measurement rinse and wipe are abbreviated as R and W, respectively.

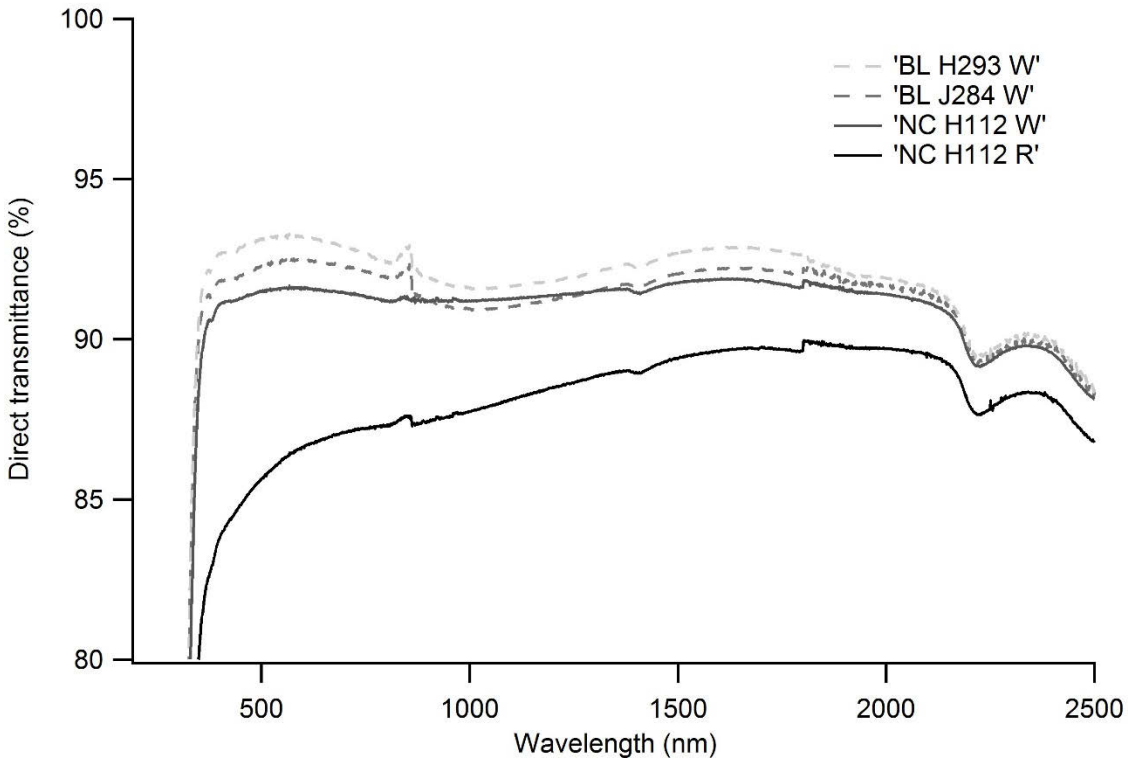

Figure 16: Direct transmittance of rinsed and wiped no-clean H (AS-coated) coupon. Unaged J (uncoated, untempered) and H coupons are shown for reference. The no-clean H coupon did not fully recover to its baseline measurement when wiped, indicating some of the coating may have been worn away. Results shown are averages of three measurements on the same coupon. In the coupon code, the cleaning practices are abbreviated as NC (no-clean), DB (dry-brush), WS (water-spray), or WSS (wet-sponge-squeegee), and compared to the baseline abbreviated as BL. Pre-measurement rinse and wipe are abbreviated as R and W, respectively.

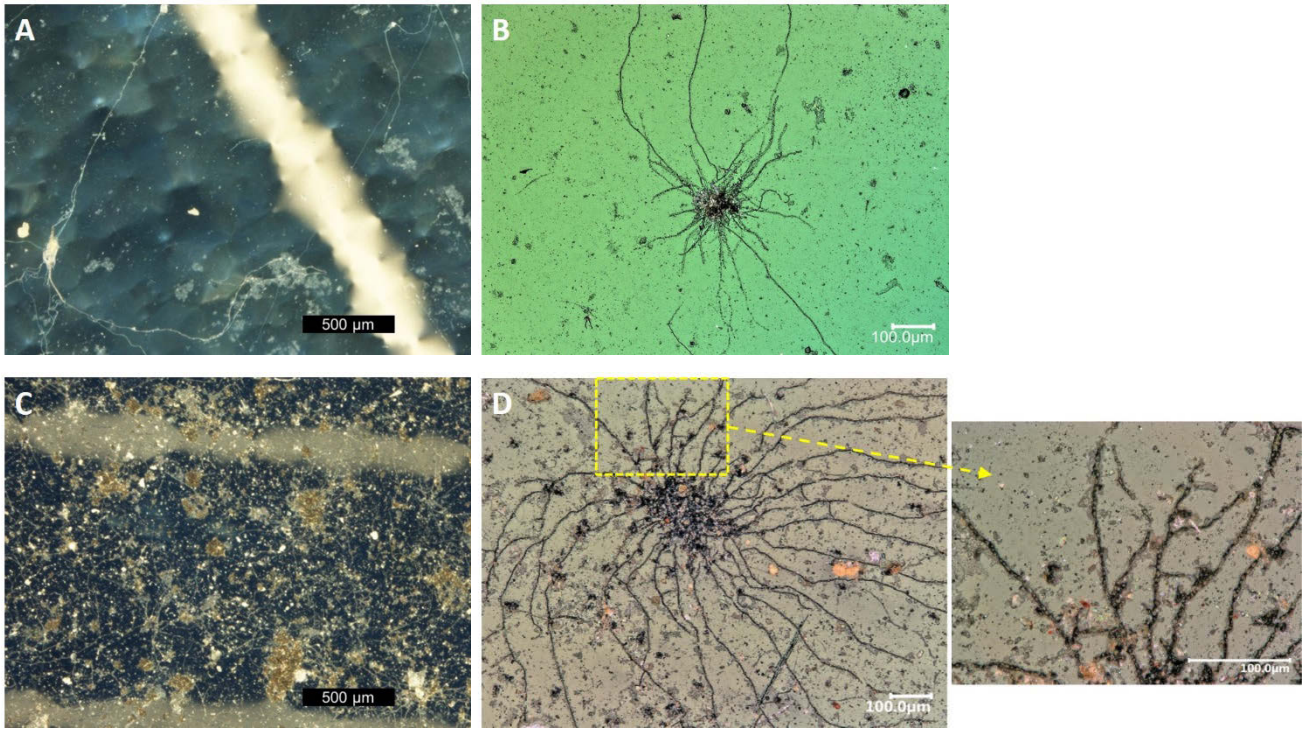

Figure 17: Micrographs of full-sized modules received after aging for 11 years in Palms, California (a), and 6 years in Argenbühl, Germany (c, d). The fungi on these modules are similar to the fungi found on the coupons in this study, such as NC J052 (b). Varying degrees of fungal contamination are seen on all surfaces, with the potential to severely reduce transmittance in more heavily soiled areas. White striations in the backgrounds of Figures 17a and 17c are bus bars under the module glass.

Tables:

Table 1. Coupon deployment locations, respective climate classifications, PM2.5 concentrations, dust storm, and precipitation information [26] [27] [28]. PM2.5 represent estimates of the average ground-level concentration (in $\mu g/m^3$) of fine particulate experienced in 2015 by each site. These data have been extracted from the 0.1-degree × 0.1-degree resolution database developed by [29].

Deployment Location: City, State (Country)	Köppen Climate Classification	General Climate Type	Average PM2.5 ($mg \times m^{-3} \times y^{-1}$)	Number Dust Storms (y^{-1})	Annual Precipitation (mm)
Sacramento, CA (USA)	Csa	Mediterranean	14.9	0	464
Tempe, AZ (USA)	BWh	Hot desert	12.6	4	204
Mumbai (India)	Aw	Tropical wet & dry	52.5	0	2,258
Dubai (UAE)	BWh	Hot desert	86.4	4	94
Kuwait City (Kuwait)	BWh	Hot desert	70.8	21	116
Argenbühl (Germany)	Cfb	Temperate oceanic	10.0	0	1,159
Palms, CA (USA)	Csa/Csb	Mediterranean	10.5	0	379

Table 2. Characteristics of all indexes of 75 × 75 mm coupons. Two types of AR coatings were used in this study: a graded index (where the refractive index was varied through thickness of the coating based on its porosity) and a single-layer interference coating (where destructive interference minimizes reflection at an optimal wavelength; i.e., a quarter-wave layer) [30]. Hydrophobicity was determined by the water contact angle; $10° < \theta \leq 55°$ was designated hydrophilic, $55° < \theta \leq 90°$ was designated weakly hydrophilic, and $90° < \theta \leq 120°$ was designated weakly hydrophobic.

Index	Substrate Material	AR Type	AS Functionality?	Hydrophobicity
A	PMMA	N/A	N/A	Weakly hydrophilic
B	Diamant	Graded index	Y	Weakly hydrophobic
D	Diamant	Graded index	Y, oleophobic	Weakly hydrophilic
E	Optiwhite	Graded index	N/A	Hydrophilic
G	Optiwhite	Graded index	Y	Hydrophilic
H	Diamant	Interference	Y	Weakly hydrophobic
J	Diamant	N/A	N/A	Hydrophilic
K	Optiwhite	N/A	N/A	Hydrophilic
T	Diamant, tempered	N/A	N/A	Hydrophilic
U	Diamant	Interference	Y	Weakly hydrophobic

Table 3. Elemental composition of the locations identified in Figure 6.

Position	Elemental Composition from EDS (%)									
	C	O	Fe	Na	Mg	Al	Si	Cl	K	Ca
1	30.7	36.1	–	5.5	1.8	0.7	21.2	0.5	0.7	2.4
2	6.4	45.6	1.4	7.2	3.5	3.1	29.8	–	–	3.1
3	20.3	38.7	–	7.0	2.1	0.8	28.0	–	–	3.1
4	10.4	43.1	–	7.7	2.4	1.2	31.9	–	–	3.4